EERC
Energy & Environmental Research Center

UNIVERSITY OF NORTH DAKOTA
15 North 23rd Street — Stop 9018 / Grand Forks, ND 58202-9018 / Phone: (701) 777-5000 Fax: 777-5181
Web Site: www.undeerc.org

March 31, 2010

Ms. Karlene K. Fine
Executive Director
North Dakota Industrial Commission
600 East Boulevard Avenue
State Capitol 14th Floor
Bismarck, ND 58505-0310

Dear Ms. Fine:

Subject: Fischer–Tropsch Fuels Development; Contract No. R003-009
EERC Funds 14729, 14730, 14731, and 14732

Enclosed for your review is the final report for the project entitled "Fischer–Tropsch Fuels Development."

If you have any questions, please contact me by phone at (701) 777-3252, by fax at (701) 777-5181, or by e-mail at jstrege@undeerc.org.

Sincerely,

Joshua R. Strege
Research Engineer

JRS/kmd

Enclosure

FISCHER–TROPSCH FUELS DEVELOPMENT

Final Report

Submitted to:

Karlene K. Fine

North Dakota Industrial Commission
600 East Boulevard Avenue
State Capitol 14th Floor
Bismarck, ND 58505-0310

Submitted by:

Joshua R. Strege
Jason D. Laumb
Joshua J. Stanislowski
Anthony C. Snyder
Michael L. Swanson

Energy & Environmental Research Center
University of North Dakota
15 North 23rd Street, Stop 9018
Grand Forks, ND 58202-9018

2010-EERC-03-10

March 2010

NDIC DISCLAIMER

This report was prepared by the Energy & Environmental Research Center (EERC) pursuant to an agreement partially funded by the Industrial Commission of North Dakota, and neither the EERC nor any of its subcontractors nor the North Dakota Industrial Commission (NDIC) nor any person acting on behalf of either:

(A) Makes any warranty or representation, express or implied, with respect to the accuracy, completeness, or usefulness of the information contained in this report or that the use of any information, apparatus, method, or process disclosed in this report may not infringe privately owned rights; or

(B) Assumes any liabilities with respect to the use of, or for damages resulting from the use of, any information, apparatus, method, or process disclosed in this report.

Reference herein to any specific commercial product, process, or service by trade name, trademark, manufacturer, or otherwise does not necessarily constitute or imply its endorsement, recommendation, or favoring by the NDIC. The views and opinions of authors expressed herein do not necessarily state or reflect those of the NDIC.

EERC DISCLAIMER

LEGAL NOTICE This research report was prepared by the EERC, an agency of the University of North Dakota, as an account of work sponsored by NDIC. Because of the research nature of the work performed, neither the EERC nor any of its employees makes any warranty, express or implied, or assumes any legal liability or responsibility for the accuracy, completeness, or usefulness of any information, apparatus, product, or process disclosed or represents that its use would not infringe privately owned rights. Reference herein to any specific commercial product, process, or service by trade name, trademark, manufacturer, or otherwise does not necessarily constitute or imply its endorsement or recommendation by the EERC.

TABLE OF CONTENTS

LIST OF FIGURES ii

LIST OF TABLES ii

EXECUTIVE SUMMARY iii

1.0 INTRODUCTION 1

2.0 BACKGROUND 3

3.0 EXPERIMENTAL APPROACH 4
- 3.1 Task 1 – FT System Testing 4
- 3.2 Task 2 – Catalytic Development and Production 5
  - 3.2.1 Process Design 5
  - 3.2.2 Production Test 1 7
  - 3.2.3 Production Test 2 8
  - 3.2.4 Silica and Potassium Impregnation 8
  - 3.2.5 Pelletizing 9
  - 3.2.6 Calcination 9
- 3.3 Task 3 – Process Simulation and Product Enhancement 9
  - 3.3.1 Process Simulation 9
  - 3.3.2 Product Enhancement 11

4.0 MAJOR FINDINGS AND DISCUSSION 12
- 4.1 Task 1 – FT System Testing 12
  - 4.1.1 Gasifier Operation 12
  - 4.1.2 FT Reactor Operation 20
- 4.2 Task 2 – Catalytic Development and Production 28
- 4.3 Task 3 – Process Simulation and Product Enhancement 28
  - 4.3.1 Process Simulation 28
  - 4.3.2 Product Enhancement 30

5.0 SUMMARY 30

6.0 REFERENCES 32

RAW DATA ..... Appendix A

DESCRIPTION OF EQUIPMENT ..... Appendix B

LIST OF FIGURES

1 Schematic illustration of catalyst production equipment 7

2 Aspen model representation of the FBG and FT reactor 10

3 Bed temperature distribution during Test FBG002 14

4 Bed temperature distribution during Test FBG003 15

5 Ambient air temperature during each week of testing 16

6 Bed temperature distribution during Test FBG004 17

7 Bed temperature distribution during Test FBG005 19

8 GC–MS results with time for Test FBG002 22

9 GC–MS results with time for Test FBG004 24

10 GC–MS results with time for Test FBG005 26

11 GC–MS peak breakdown for December 2 16:00 sample 27

12 Liquid hydrocarbon distribution: reactor data vs. model predictions 29

LIST OF TABLES

1 Major Reactions in FT Synthesis 3

2 Composition of Coal and Biomass Feeds Used in Gasification Testing 6

3 Average Run Conditions During Test FBG002 13

4 Average Run Conditions During Test FBG003 14

5 Average Run Conditions During Test FBG004 18

6 Average Run Conditions During Test FBG005 19

7 Average FT Reactor Run Conditions and Product Properties 21

8 Exit Gas Concentrations: Gasifier Data vs. Model Predictions 28

FISCHER–TROPSCH FUELS DEVELOPMENT

EXECUTIVE SUMMARY

For this Energy & Environmental Research Center project, a high-pressure fluidized-bed gasifier was coupled to a bench-scale packed-bed Fischer–Tropsch (FT) reactor. Two coal types were gasified: a North Dakota lignite and a Powder River Basin subbituminous, both of which are used in North Dakota. In addition, three biomass types were cogasified with the coal and also gasified straight: switchgrass and dried distiller's grains and solubles (DDGS) from North Dakota sources and olive pits from Greece. The olive pits were gasified because they had been pretreated as part of the project that generated the switchgrass and DDGS, and it was thought that testing this available feedstock would generate comparative data that might illustrate the relative advantages or drawbacks of the two North Dakota biomass feeds.

Syngas was cleaned by using hot sorbent beds to remove H_2S and water-cooled quench pots to remove waters and tars. The gasifier was successfully operated on all coal and biomass types. Biomass pretreatment by leaching helped to prevent ash agglomeration when cofeeding 30% biomass with coal (either subbituminous or lignite), and biomass torrefaction led to higher gasification temperatures. Untreated biomass led to agglomeration, demonstrating that leaching had helped to improve the gasification potential of the biomass. Issues with gasifier operation prevented any clear results as to whether long-term, sustainable gasification of 100% biomass (that is, without coal blending) was feasible on this system.

The packed-bed FT reactor achieved sustained liquid synthesis and temperature control, demonstrating the feasibility of this design for small-scale operation. However, catalyst deactivation was apparent both from reactor operation and product analysis. The primary cause of deactivation appears to have been oxidation due to high CO_2 concentrations. Gasification tars may also have contributed to catalyst deactivation by coking. An attempt was made to regenerate the catalyst, with no noticeable impact on catalyst activity, suggesting more than one mode of catalyst deactivation.

A process for generating kilogram-scale quantities of pelletized iron-based catalyst was conceived of, constructed, and tested. Although the process was successful, the catalyst generated by this process was produced too late to be used for testing in the packed-bed FT reactor.

Using AspenPlus™ software, a computer-based model was developed that is capable of accurately predicting the gas composition from the gasifier. Early results from laboratory-scale FT synthesis were used to generate equations for predicting the behavior of the packed-bed FT reactor. However, the syngas composition from the gasifier was sufficiently different from the composition used in the laboratory-scale reactor that the model could not accurately predict the distribution of various components in the FT liquids.

The liquid product from the packed-bed FT reactor was upgraded to improve its fuel qualities. Although not required by the proposal, the aim of the upgrading effort was to generate

specification-compliant jet fuel. The product quality was much improved by hydrotreating, but product enhancement did not fully convert the FT product into jet fuel. The effort demonstrated the feasibility of a FT product-upgrading process and also identified key issues to be considered if the goal of upgrading FT liquids is to produce jet fuel.

FISCHER–TROPSCH FUELS DEVELOPMENT

1.0 INTRODUCTION

There has been growing interest in recent years to supplant petroleum oil-based fuels with alternative transportation fuels. At the same time, increasing concern over greenhouse gas emissions is encouraging the use of renewable energy, which reduces greenhouse gas emissions because the plant matter used as feedstock reabsorbs some of the carbon dioxide emitted during combustion. There are two broad routes by which biomass can be converted into liquid transportation fuels: biologically, using microorganisms and/or enzymes to convert sugars and other plant fractions into usable fuel, and thermochemically, using gasification and other nonbiological techniques to break down and rearrange the biomass molecules. There is some overlap between these two general routes to fuel synthesis; for instance, syngas from a gasifier can be fed to a fermentor to yield ethanol [1, 2]. However, the two methods are significantly different to be classified as separate approaches.

While each general approach has advantages and disadvantages, the thermochemical route presents three near-term benefits over the biological route. First, gasifiers (high-temperature gasifiers, in particular) are relatively feedstock-agnostic. That is, they can convert any carbon-based material into syngas, provided that the feedstock has enough energy content to achieve sustained gasification. By contrast, microorganisms and enzymes are often feedstock-specific. Second, syngas chemistry can be adjusted using well-established commercial processes, while improving biofuel production from microorganisms may require years of research without fruition [3]. Third, gasification and other thermochemical approaches take advantage of the entire biomass feedstock, while most biological approaches use only sugars derived from hemicellulose and part of the cellulose (leaving the remaining cellulose and lignin fractions of biomass unconverted) [4]. All of these issues with the biological route may be overcome as research progresses, but in the immediate future, thermochemical conversion appears to be more favorable.

Although thermochemical pathways offer many near-term advantages over biological routes to renewable synfuels, one of the most well-established thermochemical pathways to generate liquid fuel (gasification followed by Fischer–Tropsch [FT] synthesis) has at least two major issues remaining to be overcome before it can be applied to biomass on a large scale. First, many biomass types are rich in alkali and chlorine, species that cause agglomeration and corrosion, respectively. Finding ways to remove or minimize the impact of these species will be critical to incorporating biomass into gasifiers designed for coal or petroleum residues [5, 6]. Second, gasification and FT synthesis do not readily scale down. Biomass gasification plants are likely to be limited in scale to the amount of biomass available in the immediate area [7, 8]. Given the massive infrastructure required to not only gasify the biomass but then to shift the gas chemistry, clean the syngas, and convert the gas to liquid fuels, gasification and FT synthesis will likely require a larger plant than can be supplied at a reasonable collection radius in order to operate at a profit.

There are three clear ways by which FT synthesis could be made more economical for biomass gasification. First, the operating and capital costs could be lowered by reducing process complexity, allowing a smaller-scale plant to operate at a profit. Capital cost is especially important for small-scale plants because capital costs usually do not scale linearly with plant size, meaning a small plant costs much more per unit capacity than does a larger plant. Second, biomass could be supplemented with a nonrenewable feedstock such as coal, allowing a larger plant to be built without requiring an unacceptably large biomass collection radius. Third, off-site biomass could be densified, making it more economical to transport over a long distance and thereby expanding the collection radius.

One of the most capital-intensive and complex units in a gas-to-liquids plant is the gas cleanup train. In large-scale commercial gasifiers, syngas is often cleaned using cold-gas solvents such as Rectisol™ or Selexol™. Such solvent-based processes cool the syngas to subzero temperatures so that the solvent can physically absorb gas species such as carbon dioxide (CO_2) and hydrogen sulfide (H_2S). H_2S is of special concern in the FT process because it is known to rapidly and permanently deactivate FT catalysts. Because of the need for cryogenic cooling, the capital and operating costs for traditional cold-gas cleanup are significant. If H_2S and other key contaminants can be removed using hot-gas sorbents rather than cold-gas solvents, the capital and operating costs for gasification and FT synthesis can be greatly reduced [9, 10].

The second method by which biomass gasification economics can be improved is by supplementing biomass with coal. Unlike biomass [11], coal is available year-round, and there are decades of commercial operating experience in converting coal into syngas and transportation fuels. However, some coal components (such as aluminosilicates) may interact unfavorably with biomass components (such as sodium or potassium), leading to agglomeration. Some biomass components, in particular chlorine, may also lead to corrosion. As such, it may be necessary to remove agglomerating and corroding species from the biomass prior to gasification [5, 6, 12, 13].

The final method by which biomass gasification can be made more economical is by densifying the biomass at the collection site. Numerous options are available, including drying, pelletizing, pyrolysis, and torrefaction. In cofeeding with coal for gasification, torrefaction offers a unique advantage in that the torrefaction product is similar in energy density and physical characteristics to coal, allowing it to achieve similar bed temperatures and to be fed similarly [14]. Cofeeding torrefied biomass with coal will likely be an easier proposition than cofeeding raw biomass or pyrolysis oil into a gasifier.

One last nontechnical limitation to developing small-scale FT systems is catalyst procurement. Many catalyst vendors have prohibitively high royalty fees or exclusive licensing agreements with larger companies, making it difficult for smaller entities to procure FT catalyst. As such, aside from the research needs mentioned above, there is also a potential need to develop processes for producing FT catalyst using off-the-shelf equipment and straightforward techniques available from the open literature.

2.0 BACKGROUND

The FT process is used to convert synthesis gas (syngas), which primarily comprises carbon monoxide (CO), hydrogen (H_2), CO_2, and water (H_2O), into hydrocarbons. This process was developed in the 1920s by German scientists Franz Fischer and Hans Tropsch and was quickly commercialized, producing 4.1 million barrels, or 10%–15% of Germany's synthetic fuel production, in 1944 [15]. In subsequent decades, interest in FT synthesis has varied according to national and environmental concerns, technological advances, and perhaps most importantly, the price of crude oil.

Within a FT reactor, products are formed through several pathways, listed in Table 1. The second reaction listed is a simplified model of the synthesis of hydrocarbon chains, a polymeric synthesis in which the monomer is methylene ($-CH_2-$). Generally, this reaction produces paraffinic straight-chain alkanes ranging in length from C_1 to C_{50}, along with smaller amounts of isomerized (i.e., not straight-chain) hydrocarbons, olefins, and light alcohols. Other reactions listed here represent side reactions in the reactor; these include methanation (Reaction 1), the water–gas shift reaction (Reaction 3), and the Boudouard reaction (Reaction 4), which forms carbonaceous deposits leading to the deactivation of the catalyst.

FT reactions are typically catalyzed in the presence of cobalt or iron. Typically cobalt-based catalysts are used to catalyze syngas having a H_2:CO ratio of about 2.0–2.3, which is comparable to syngas derived from natural gas. Iron-based catalysts are used to catalyze syngas having a H_2:CO ratio of about 0.5–1.3, which is comparable to syngas derived from coal gasification [16]. Iron also catalyzes the water–gas shift reaction (Reaction 3, Table 1), which makes up for the stoichiometric hydrogen deficiency in the lower-hydrogen-ratio syngas blends by converting excess CO and H_2O into hydrogen.

There are several measures by which a FT catalyst can be judged. Perhaps the simplest measure is the production rate of liquids. Obviously, the more active and selective a FT catalyst, the more liquid it will produce. However, a simple production rate can be deceiving because other factors (syngas composition, flow rate, etc.) can cause the production rate to go up or down. A second simple measure of catalyst performance is the weight ratio of liquid organic products to aqueous products. If a catalyst begins to produce a significant amount of light gas, more water will be generated, while the amount of liquid hydrocarbon will decrease. Thus organic:aqueous ratio is a measure of catalyst selectivity.

A third indication of catalyst performance is conversion, a measure of what percentage of the reactant (CO or H_2) is converted into product. Conversion as defined here accounts only for

Table 1. Major Reactions in FT Synthesis

$CO + 3H_2 \leftrightarrow CH_4 + H_2O$	(1)
$nCO + (2n+1)H_2 \rightarrow (1/n)CnH_{2n+2} + nH_2O$	(2)
$CO + H_2O \leftrightarrow CO_2 + H_2$	(3)
$2CO \leftrightarrow C + CO_2$	(4)

the activity of the catalyst, not whether it is generating useful product. A fourth measure of catalyst performance is selectivity to light gas, abbreviated in this report as STLG. This is a measure of what percentage of the consumed CO is converted to light gas such as methane or ethane, which are considered undesirable by-products. The higher the conversion, the more active the catalyst; the higher the STLG, the less selective the catalyst. The formulae for both conversion and STLG are provided below, with all values taken as mole percents. It should be noted that outlet concentrations are multiplied by the ratio of outlet-to-inlet N_2 to scale them to inlet concentrations. Because gas is consumed, mole percents are not indicative of molar flow rates, and scaling by the change in inert gas concentration is necessary to correct outlet flows to inlet flows. Taken together, these four indicators (production rate, organic:aqueous ratio, conversion, and STLG) are used in this report to assess catalyst performance.

$$\text{Conversion(CO)} = \frac{CO_{in} - CO_{out} \times \frac{N2_{in}}{N2_{out}}}{CO_{in}} \qquad \text{[Eq. 1]}$$

$$\text{STLG} = \frac{\left(CH4_{out} + HC_{out}\right) \times \frac{N2_{in}}{N2_{out}} - \left(CH4_{in} + HC_{in}\right)}{CO_{out} \times \frac{N2_{in}}{N2_{out}} - CO_{in}} \qquad \text{[Eq. 2]}$$

3.0 EXPERIMENTAL APPROACH

3.1 Task 1 – FT System Testing

A thorough description of the major equipment used for this Energy & Environmental Research Center (EERC) project is provided in Appendix B. The desulfurization transport reactor, which has been operated successfully numerous times over the course of several years [17], was found to have been damaged when it was coupled to the new gasifier and was not used for sulfur removal in any of the testing in this project. Instead, two of the fixed beds were loaded with regenerable RVS-1® commercial sulfur sorbent, and two downstream beds were loaded with nonregenerable ActiSorb®S2 polishing sorbent to capture remaining traces of sulfur compounds from the syngas. Both sorbents were purchased from Süd-Chemie. Each set of fixed beds was operated one at a time so that spent sorbent from one bed could be regenerated or replaced while the system was still running on the second bed.

Four continuous test periods were conducted on the fluid-bed gasifier (FBG), each lasting approximately 1 work week (4½ days). During the first two test periods, a Powder River Basin (PRB) subbituminous coal was gasified. This coal was selected because it was immediately available, was likely to be a fairly benign coal in terms of gasification behavior, and is used in North Dakota. During the second two periods, North Dakota lignite from the Falkirk Mine was gasified. In each test, several biomass samples were cofed with the coal, and at several times, the feed was switched to 100% biomass. The biomass types included switchgrass from the North Dakota State University (NDSU) Agricultural Experiment Station in Streeter, North Dakota; dried distiller's grains and solubles (DDGS) from the Archer Daniels Midland corn bioethanol

plant in Walhalla, North Dakota; and olive pits from Greece. The olive pits were selected because the biomass preparation effort was funded mostly under a separate project with a potential interest in this feed.

All of the biomass samples were pretreated by leaching to remove the alkali metals, chlorine, phosphorus, and sulfur to avoid ash-related problems during the gasification process as well as to avoid potential catalyst poisoning during the FT process. In addition, a portion of the olive pits were torrefied to increase the heating value, and a portion of the DDGS was left untreated to examine the relative impact of gasifying treated versus nontreated biomass. Table 2 provides analytical data for each of these feeds, with "TL" indicating "torrefied and leached."

Syngas exiting the gasifier quench pots was analyzed online by laser gas analysis (LGA), gas chromatography (GC) coupled to thermal conductivity detectors (GC–TCD), and GC coupled to a pulsed-flame photometric detector (GC–PFPD) for ultralow sulfur detection. After steady-state gasification had been achieved and the sulfur capture fixed beds brought online, H_2S in the syngas would fall exponentially to below Dräger tube (and, in some cases, below GC–PFPD) detection limits over the course of several hours. Once H_2S had dropped below 1 ppmv as measured by Dräger tube, clean, dry syngas was passed to the FT system. It was necessary to wait until H_2S had dropped so low because H_2S is a strong FT catalyst poison.

Both fixed-bed FT reactors were loaded with iron-based catalyst. During the first 2 weeks of testing (Tests FBG002 and FBG003), only one fixed-bed reactor was used. This left the other loaded reactor available in the event that the first reactor was overheated or deactivated as a result of sulfur breakthrough from the upstream sorbent beds. During the second 2 weeks of testing, both reactor beds were used in an attempt to increase the amount of FT product recovered. Product gas exiting the FT reactor was continuously monitored by a second LGA.

At the start of the project, it was anticipated that the EERC would not be able to obtain commercial FT catalysts, and so one of the tasks in this project was catalyst development (Section 3.2). However, the catalyst developed under Task 2 was not ready in time for FT system testing, so a large batch of an existing EERC iron-based catalyst formulation was instead produced and used for Task 1.

3.2 Task 2 – Catalytic Development and Production

3.2.1 Process Design

As mentioned in Section 3.1, Task 2 was initially conceived of as a way for the EERC to perform FT testing without the need to procure catalyst from vendors with prohibitively high royalty fees or exclusive licensing agreements with larger commercial companies. The process design was based on coprecipitation in a flowing reactor with a planned production of 1 kg of catalyst per run. Two 15-gal closed-head drums held the Fe–Cu reagent and the base. They were placed inside open-head 30-gal drums, which served as containment. A third closed-head 30-gal drum served as a deionized water reservoir for mixing the solutions and flushing the system. Two peristaltic pumps were used to introduce the reagent and base to the reactor. The pumps were cross-connected to the water reservoir to allow flushing the reactor system and for metering

Table 2. Composition of Coal and Biomass Feeds Used in Gasification Testing

	PRB Antelope Coal	ND Lignite	Treated Olive Pits	TL Olive Pits	Treated DDGS	Treated Switchgrass	DDGS
Leached?	No	No	Yes	Yes	Yes	Yes	No
Torrefied?	No	No	No	Yes	No	No	No
Air-Drying Loss	16.62	14.90	44.40	39.40	22.00	59.60	0.40
Proximate Analysis (all values reported as weight percent as determined)							
Moisture	6.94	10.00	9.39	5.70	10.57	4.87	7.12
Volatile Matter	42.32	32.52	62.78	43.27	65.47	63.69	69.01
Fixed Carbon	43.85	43.88	24.70	47.44	21.43	16.54	19.99
Ash	6.89	13.61	3.13	3.58	2.53	14.90	3.88
Ultimate Analysis (all values reported as weight percent as determined)							
H	4.86	4.97	6.65	5.29	7.40	6.46	7.14
C	82.83	55.49	50.16	66.66	49.02	44.11	48.31
N	1.17	0.87	1.60	1.43	4.28	1.21	3.66
S	0.38	1.38	0.13	0.11	0.34	0.20	0.39
O	3.87	23.68	38.33	22.93	36.43	33.12	36.58
HHV[1], Btu/lb	10,550	9246	8282	10,994	8584	6750	8532
CCV[2], Btu/lb	14,611	9646	9060	11,504	9290	8279	9078
Ash Analysis (all values reported as weight percent on an ash basis)							
SiO_2	32.6	40.5	6.6	10.1	3.0	40.4	5.2
Al_2O_3	15.0	13.8	1.5	2.6	0.8	1.5	0.0
Fe_2O_3	7.48	7.57	1.80	3.72	0.60	2.14	0.43
TiO_2	1.17	0.49	0.11	0.18	0.04	0.12	0.02
P_2O_5	1.08	0.28	2.10	3.59	43.12	1.93	39.65
CaO	21.3	16.1	51.7	54.9	23.5	40.0	1.9
MgO	5.86	5.12	0.77	3.22	6.10	2.86	13.41
Na_2O	0.84	0.89	0.03	0.91	3.95	0.23	5.26
K_2O	0.56	1.35	0.68	13.24	13.47	5.26	30.68
SO_3	13.25	13.32	1.78	4.73	4.70	1.47	2.84
Cl	0.00	0.00	0.10	0.08	0.55	0.12	0.64
Unknown	0.00	0.00	32.63	0.73	0.00	3.80	0.00

[1] Higher heating value.

[2] Calculated calorific value.

water when mixing the chemicals. Counters added to the pump motor shafts recorded the pump revolutions. Pumping test results showed that total flow could be measured from the total revolutions to within 1.5%. The reagent and base flowed from the pumps through two preheaters to bring their temperatures to the desired 82°C. Temperature was maintained by internal rod heaters and controllers. The reagent and base were mixed in the reactor, which was also heated. A stirrer provided the required mixing. The pump metering the base was manually adjusted to control the pH measured in the reactor. The precipitated product was continuously drained from an overflow outlet near the top of the reactor through a water-cooled heat exchanger for filtering. The washing step, the silication step, and the potassium impregnation step were batch processes carried out in the collection drum. A schematic and illustration of the precipitation process equipment is shown in Figure 1.

3.2.2 Production Test 1

The first catalyst production test used Fe–Cu solution precipitated with K_2CO_3. The Fe–Cu flow was initially set at a slow flow rate of approximately 50 mL/minute and the pH adjusted to between 7 and 8 by adjusting the K_2CO_3 flow. Difficulty was encountered with controlling the pH because of the slow response of the electrode.

Severe frothing soon occurred in the reactor, with the solution overflowing several times. The condenser line also became plugged several times. The frothing, overflow, and plugging required interrupting the test until the situation was remedied. In retrospect, it was deduced that the frothing was the result of the generation of CO_2 from the carbonate solution when the pH dropped below 8. This was exacerbated by the 82°C solution temperature and the vigorous stirring of the solution. The use of K_2CO_3 as a base was thus found to be not ideal for the precipitation reaction. The test was terminated after approximately 45 minutes, with 525 mL of Fe–Cu solution and 485 mL of K_2CO_3 fed.

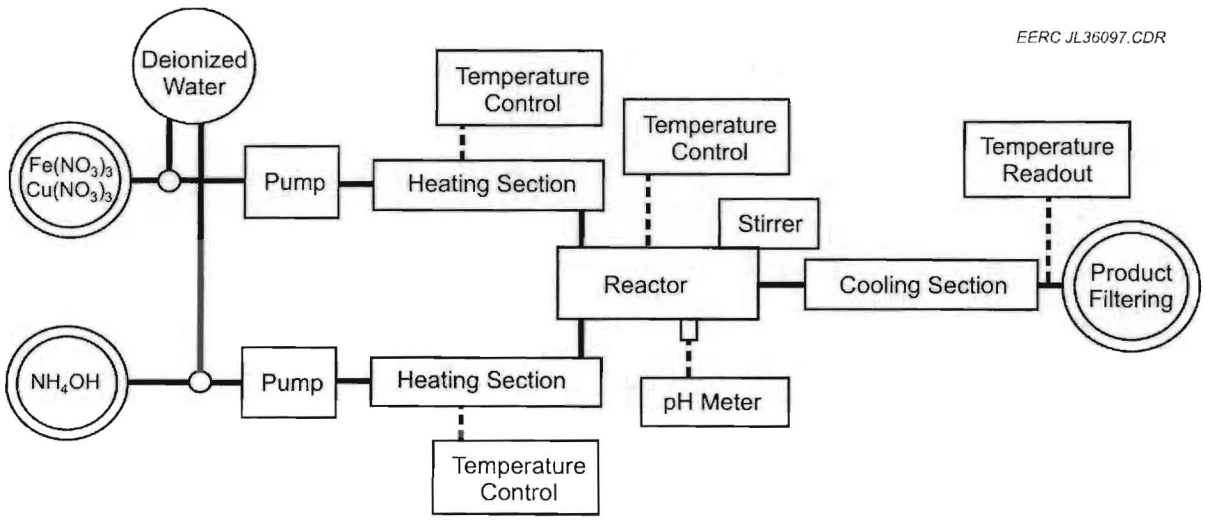

Figure 1. Schematic illustration of catalyst production equipment.

Vacuum filtering of the precipitate was done with a Buchner funnel holding 24-cm-diameter FPR 240 paper filters. Initially, the precipitate was collected in the funnel directly from the condenser. This proved to be impractical since the filtering proceeded very slowly. After the funnel was filled to capacity, additional precipitate was collected in a separate container for later filtering.

The collected product was filtered the next day and rinsed with three 1-liter batches of deionized water. Again, the filtering process was extremely slow, although allowing the precipitate to settle and decanting the clear liquid portion to filter first was of some benefit. A total of 501.9 grams of wet product was obtained. Drying a small (3.1-gram) sample indicated that the product contained approximately 77% water. The dry product obtained was thus approximately 113 grams. The wet product was found to be quite sticky and difficult to handle and transfer.

3.2.3 Production Test 2

The second catalyst production test used Fe–Cu solution precipitated with KOH. The Fe–Cu flow was initially set at a slow flow rate of approximately 50 mL/minute and the pH adjusted to between 7 and 8 by adjusting the KOH flow. Again, difficulty was encountered with controlling the pH because of the slow response of the electrode. No frothing occurred during the test. The second test ran until the supply of KOH was depleted. Approximately 4500 mL of the Fe–Cu solution and 8600 mL of KOH were fed. The precipitated product was collected in 1-gallon (4-liter) plastic buckets for subsequent filtering after settling. The solution pH of each was tested, and additional KOH added until basic (pH = 8). After allowing time for settling, the filtration and washing were performed.

The precipitate was filtered out of solution using a Buchner funnel, as in Test 1. The filtered "mud" was then slurried with approximately 3 times its weight in water. This slurry was then filtered again using the Buchner funnel.

3.2.4 Silica and Potassium Impregnation

After filtration, Cab-o-sil (SiO_2) and potassium hydrogen carbonate were added to the precipitate. 10 grams of SiO_2 and 7 grams of $KHCO_3$ were added for every 96 grams of precipitate. The first batch of catalyst that was made using potassium carbonate had to be disposed of because of contamination by other chemicals.

To prepare the second batch of catalyst, 960 grams of precipitate was mixed with 100 grams of Cab-o-sil and 70 grams of $KHCO_3$. This mixture was slurried with water in a large beaker. The beaker was placed in an oven at 50°C for several hours so that excess moisture would evaporate until the catalyst mixture had the consistency of mud.

3.2.5 Pelletizing

Several different techniques were tried for pelletizing the catalyst. One technique involved using a household cookie press with a custom-made 2-mm quadrate end. This technique did not produce a product with a consistent shape.

A second technique involved using a syringe with a small opening in the tip. The catalyst was extruded into lines on a cookie sheet, and these lines were scored to the desired length. This process was not consistent enough. The main problem was that the lines varied greatly in width.

The third and most successful technique involved spreading the catalyst onto perforated metal plates. The plates were ⅛ in. (3.2 mm) thick and the holes had a diameter of 3/16 in. (4.76 mm). This produced pellets that were approximately 3 mm thick, with a diameter of 4.7 mm before drying. The plates were filled by spreading the catalyst on with a spatula to ensure that all holes were filled. Excess catalyst was scraped off, and the plates were placed on trays and left to dry at 50°C in an oven for several hours. As the excess moisture in the pellets evaporated, the pellets shrank and fell out onto the tray below. This process produced a consistently shaped product and was easily repeatable. After the pellets had air-dried for several hours, they were sifted to remove fine particles. The pellets were then dried in an oven at 120°C for 16 hours.

3.2.6 Calcination

The catalyst was cooled and then placed in a Pyrex pan. The pan was heated at 60°C for 1 hour, 190°C for 1 hour, and finally 270°C for 8 hours. The catalyst did not crack or visibly change appearance during the calcination process. The finished catalyst product had a diameter of 3 mm and a thickness of 2 mm when the calcination process was completed.

3.3 Task 3 – Process Simulation and Product Enhancement

3.3.1 Process Simulation

A computer-based process model of the gasifier, cleanup train, and FT system was constructed using AspenPlus™ software. The model was built to simulate gasification on the EERC's FBG. A screenshot of the AspenPlus model is shown in Figure 2. Coal enters into the model as a nonconventional component. The user specifies the proximate analysis of the fuel on an as-fired basis and the ultimate analysis of the fuel on a dry basis. The analytical results are used to convert the coal stream into a stream consisting of basic elements, including C, H, N, S, and O, that can be utilized in Aspen Plus. The conversion occurs in the decomposition block with the aid of a user-provided code. The basic elements then combine with oxygen, steam, purge, and the recycle stream in the gasifier.

The FBG is simulated as two separate sections: the fluid bed and the freeboard. A phase and chemical equilibrium model called RGIBBS is used in each section to determine the products of gasification. Carbon conversion is limited in each section by user input based on data from the reactor. A solids-handling block separates the solids exiting the fluid bed by particle-size distribution. The larger-sized portion of the solids is sent back to the fluid-bed section, while

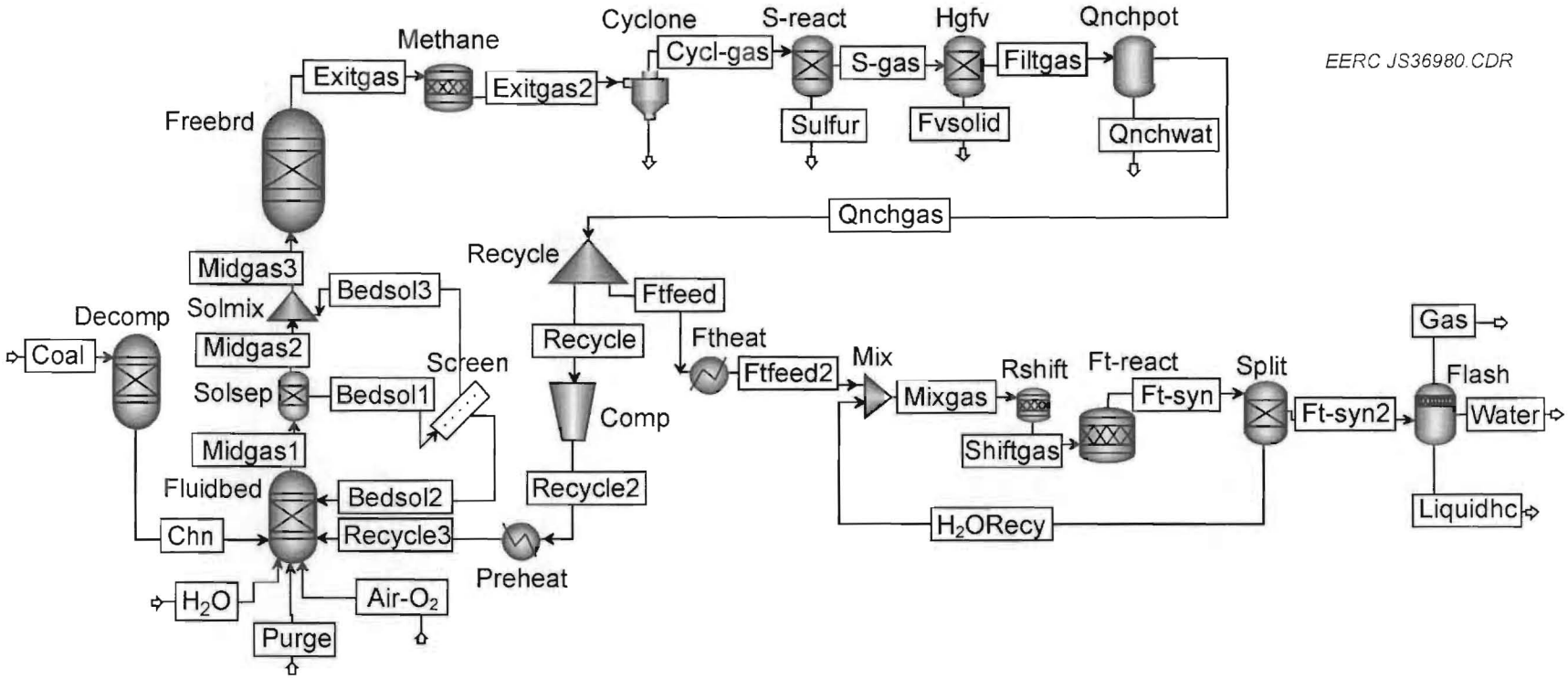

Figure 2. Aspen model representation of the FBG and FT reactor.

the smaller-sized fraction escapes to the freeboard. This feature was added to allow improved modeling of carbon conversion. However, carbon conversion modeling was never fully implemented because it was outside of the project scope and was limited by budget and time constraints. A methane reactor was added after the freeboard section because an equilibrium model is unable to predict methane presence in the gas stream at the operating temperature of the gasifier. The concentration of methane leaving the reactor is based on the actual operating conditions. The reactor also allows for the user to specify the water–gas shift reaction to further calibrate the model to operating data. This compensates for the small amount of water–gas shift that occurs in the cyclone and exit piping before the gas cools below 1000°F.

The cyclone block uses a simulated cyclone model to remove the larger particulate from the gas stream. The cyclone model is based on the geometry of the cyclone used with the FBG. The sulfur is removed in the gas stream with a component separator and does not utilize capture equations. The remaining particulate is captured in the hot-gas filter vessel (HGFV) block. The quench pot (QNCHPOT) block simulates a cooling of the gas and uses a two-phase flash to calculate the amount of water removed from the gas stream. The gas flows to a recycle splitter where a portion of the gas is fed to the FT reactor and the remaining gas is compressed, reheated, and sent back to the gasifier.

Feed gas to the FT reactor first passes through a heater that simulates the preheater found on the EERC's FT reactor. The FT reactor itself is represented by four blocks that, combined, represent one unit operation. In a FT reactor with an iron-based catalyst, significant water–gas shift occurs simultaneously with the FT reactions. The water–gas shift reactions consume water, and the FT reactions produce water. In the Aspen model, these steps must be modeled separately, and in order to maintain a proper mass balance, 50% of the water generated in the FT reactor is recycled back to the shift reactor. The shift reactor is set to shift the gas to a 2:1 H_2:CO ratio. The FT reactor uses an RSTOICH model in AspenPlus along with a calculator block to determine the products of the reaction. The Anderson–Schulz–Flory (ASF) model is used to determine the product distribution. Three separate ASF models are used: one for alkanes, one for olefins, and one for alcohols. The user is required to enter a chain growth probability value (α value) for each product type as well as the CO conversion for each product. The overall concentration of alkanes versus olefins and alcohols was determined from analyzing the product from laboratory tests but is left as a user-specified input that can be modified. In the last step of the AspenPlus model, the product from the FT reactor is cooled and separated into gas, water, and organic liquids.

3.3.2 Product Enhancement

Although the proposal for this project did not require it, the EERC's goal for product enhancement was to produce fungible jet fuel. The organic FT product derived from PRB coal during the first week of testing (Test FBG002, August 24–28) was combined for hydrotreating and distillation. The product derived from blended coal and biomass was kept separate and did not undergo product enhancement. The hydrotreating catalysts used for enhancement were supplied from a commercial source that is in the process of developing these catalysts, so no detailed process information is given here in the interest of confidentiality. The general purpose of the hydrotreating was to saturate FT liquids and to isomerize the mostly unbranched carbon chains in the FT liquid into branched carbon chains. Isomerization is necessary to meet jet fuel

specifications. The hydrotreated product was distilled and analyzed to determine density, freeze point, and product distribution, which are all key criteria for synthetic military jet fuel (JP-8).

4.0 MAJOR FINDINGS AND DISCUSSION

4.1 Task 1 – FT System Testing

4.1.1 Gasifier Operation

As is typical with new reactor systems, various design and operational issues were not discovered until the gasifier was started for the first time (i.e., during shakedown). As a result, no useful data were collected in the initial shakedown run (Test FBG001), and the first test for which results are given is Test FBG002.

Because of the large amount of data collected, it would be prohibitive to include every chart in the main body of the report. Instead, most of the results are summarized as figures in Appendix A.

4.1.1.1 Test FBG002

Table 3 provides average run conditions for Test FBG002. It should be noted that starting times do not always correlate to test durations, as any time that coal feed was off is not counted in the test duration. As can be seen, operating conditions were similar for all of the feeds. Feed rate was lower with the 30% switchgrass blend because the fuel has a lower density. Figure 3 shows the bed temperature distribution during testing. As can be seen, temperatures dropped and spiked several times during the week. This was primarily the result of brief losses in coal feed. Most of the coal feed losses were due to cyclone plugging; bed velocity was too high, and large solids were carried up into the line going to the cyclone and caused plugging. Despite these numerous upsets, temperatures were fairly stable for most of the run, including when treated biomass was added to the feed. Bed temperatures actually improved when 30% torrefied and leached olive pits were added, which is not surprising given the high heating value of torrefied pits shown in Table 2.

The temperatures began to diverge late on the final day of testing, when 30% untreated DDGS was added to the feed. This temperature divergence indicated that the bed was not fluidizing well, which implied that it was beginning to agglomerate. When the reactor was taken off-line, the bed material was found to contain many large chunks indicative of agglomeration. These results demonstrate that untreated DDGS led to agglomeration after only 2.5 hours of operation, while no signs of agglomeration were present when biomass was pretreated by leaching. Apparently the leaching process was sufficient to allow 30% biomass to be blended with PRB coal.

Table 3. Average Run Conditions During Test FBG002

Feed:	PRB Coal	30% Leached Olive Pits	30% TL Olive Pits	30% Leached DDGS	30% Switchgrass	30% DDGS
Bed Temperature, °F	1510	1505	1528	1522	1526	1500
Freeboard Temperature, °F	1542	1552	1564	1563	1561	1557
Feed Rate, lb/hr	7.0	6.8	7.1	7.4	5.0	5.6
Gas, scfh						
Recycle	403	427	418	409	410	424
Steam	334	409	409	407	407	408
Nitrogen	16	0	0	0	0	0
Oxygen	55	58	58	58	58	58
Purge	321	377	346	349	350	346
Outlet	134	78	57	50	54	112
Bed dP, in. H_2O	31	25	23	22	25	20
Freeboard dP, in. H_2O	11	7	5	7	8	10
Distributor Plate Pressure, psig	323	326	325	326	326	327
Bed Pressure, psig	305	309	308	309	309	309
Freeboard Pressure, psig	304	307	307	307	307	308
Start of Test dd/mm hh:mm	8/24/2009 10:58	8/27/2009 17:00	8/27/2009 23:49	8/28/2009 3:19	8/28/2009 10:02	8/28/2009 14:28
Test Duration, hh:mm	73:11	6:49	3:30	6:43	4:26	2:29

4.1.1.2 Test FBG003

Because of anticipated budget and time constraints, two projects shared the gasifier during Test FBG003 in order to minimize the cost and time required for each project. As a result, only a portion of the syngas was sent to the FT reactor, with the remainder being sent to a thermal oxidizer for unrelated testing. Similarly, process conditions were selected to produce enough syngas of sufficient quality to feed both the FT reactor and the thermal oxidizer, which is the reason for the elevated feed rates and system pressures in Table 4.

PRB coal was again used as the gasifier feedstock in Test FBG003 and was run for the majority of the test duration to ensure stable gasifier operation and steady flow to both the FT reactor and the thermal oxidizer. After the thermal oxidizer was taken off-line, feed was switched to 100% treated DDGS for 4 hours, then to 100% treated olive pits.

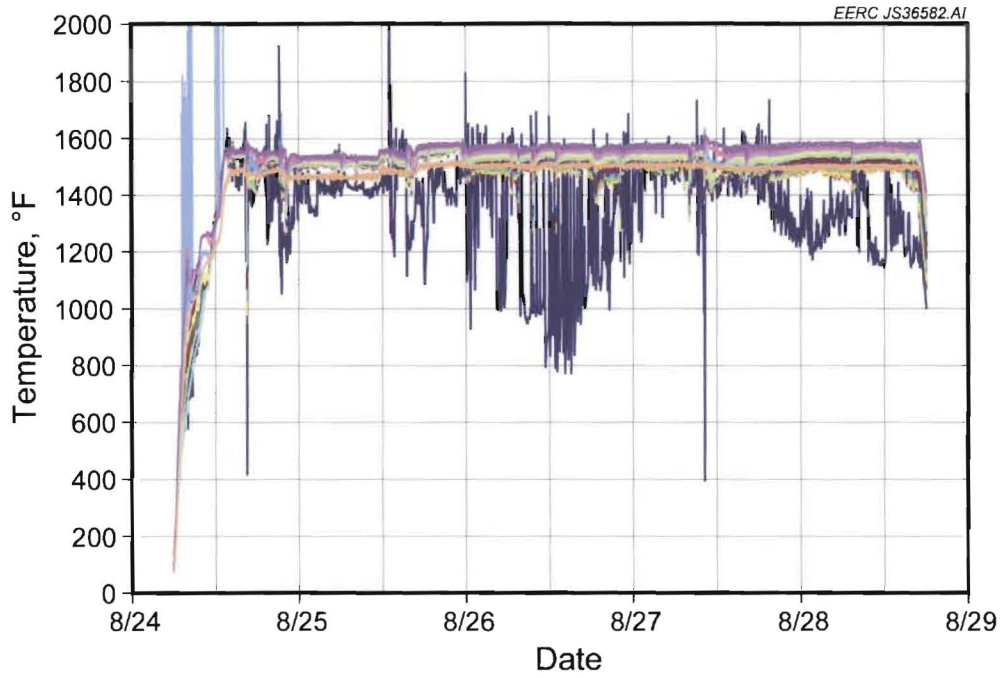

Figure 3. Bed temperature distribution during Test FBG002.

Table 4. Average Run Conditions During Test FBG003

Feed	100% PRB	100% DDGS	100% Olive Pits
Bed Temperature, °F	1539	1461	1537
Freeboard Temperature, °F	1552	1565	1555
Feed Rate, lb/hr	11.4	12.4	21
Gas, scfh			
Recycle	542	468	363
Steam	387	389	378
Nitrogen	26	23	45
Oxygen	81	78	73
Purge	227	269	285
Outlet	243	382	354
Bed dP, in. H_2O	28	53	63
Freeboard dP, in. H_2O	7	24	37
Distributor Plate Pressure, psig	526	473	516
Bed Pressure, psig	493	470	486
Freeboard Pressure, psig	491	473	473
Start of Test	9/8/2009	9/11/2009	9/11/2009
dd/mm hh:mm	11:00	9:10	13:18
Test Duration, hh:mm	68:32	4:08	0:58

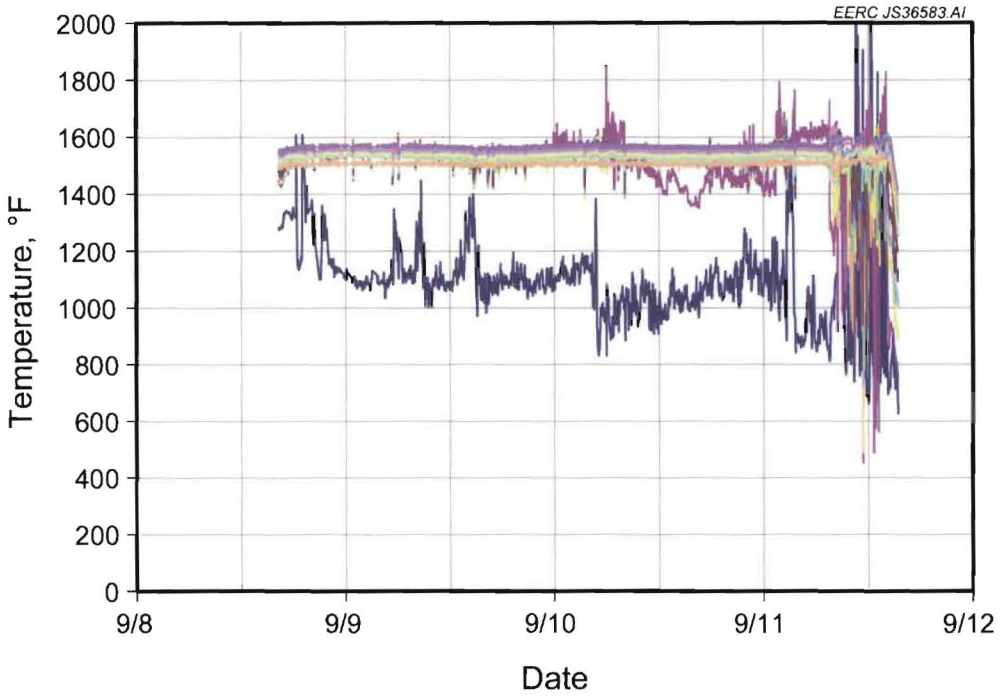

Figure 4. Bed temperature distribution during Test FBG003.

The results shown in Table 4 are misleading, as they imply that bed temperature dropped significantly when the feed was switched from PRB coal to treated DDGS and that the bed differential pressure and freeboard pressure drops rose significantly. In fact, the gasifier suffered a major upset 1.5 hours before the DDGS feed was started, and it had to be taken off-line for 1 hour and 15 minutes to clear a plug in the cyclone. This can be seen in Figure 4 at 7:40 on September 11 as a sudden drop in bed temperatures, as well as in various figures in Appendix A. As a result of the loss in fluidization during this upset, the bed had already begun to agglomerate when DDGS feed was started. As such, it is difficult to say what effect the 100% DDGS feed had on system performance in Test FBG003. The situation is exacerbated for the 100% olive pit feed, as the bed fully agglomerated after less than an hour of run time; for the same reason, most of the data for olive pits in Table 4 are unreliable. Whether either biomass contributed to rapid agglomeration is uncertain, as the cyclone plug that occurred prior to the start of biomass feed was quite severe and nearly stopped the test.

4.1.1.3 Test FBG004

During Test FBG004, the gasifier performed much more poorly than in previous tests. In particular, the recycle syngas flow rate was highly erratic, and the back-pressure control valve did a poor job at controlling system pressure. As will be discussed in Section 4.1.2.3, flow to the FT reactor was also erratic. The primary reason for this decrease in performance appears to have been a drop in outside air temperatures compared to previous tests, as shown in Figure 5. Center lines represent weighted average temperatures for the week, while the boxes above and below

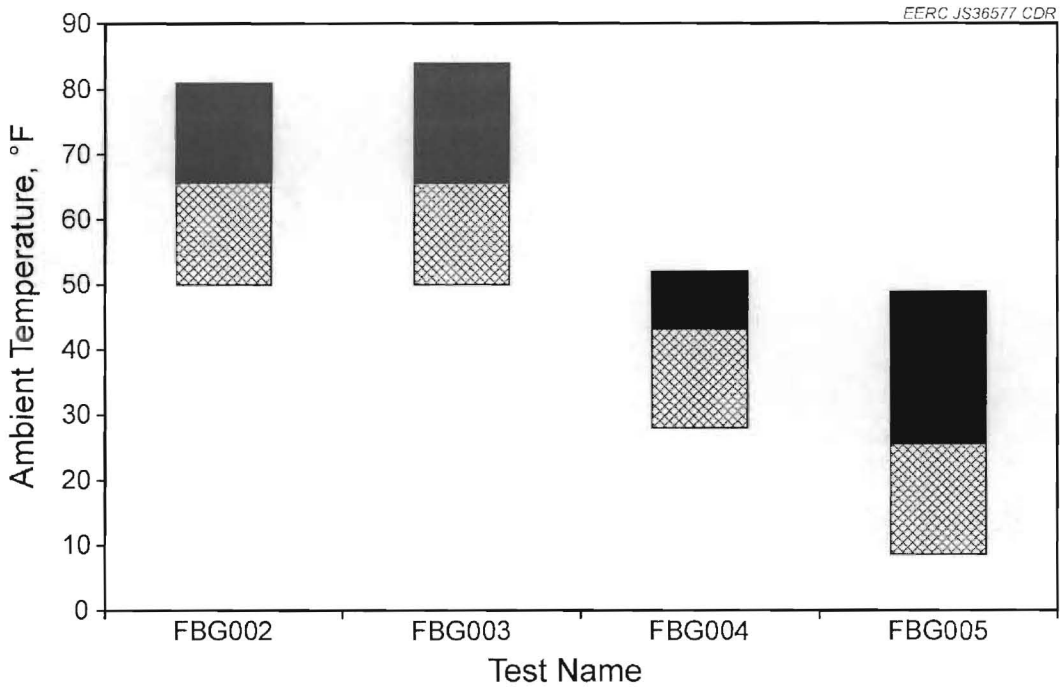

Figure 5. Ambient air temperature during each week of testing.

represent maximum and minimum temperatures, respectively. As can be seen, the maximum air temperature (52°F) in Test FBG004 was almost lower than the lowest temperature observed previously (50°F); the average temperature was more than 20°F lower (43°F in Test FBG004 as compared to 66°F in both Tests FBG002 and FBG003); and the minimum temperature was below freezing.

As a result of the lower ambient air temperatures, water and tars tended to condense in cooled, exposed lines, particularly those downstream of the gasifier's water-cooled quench pots. The gasifier is housed inside of a building, but the room temperature in the gasifier area is generally much closer to outdoor temperatures than in the control room and laboratories. Although the bulk of the water and tars was captured in the quench pots, the small amount that was able to slip through uncondensed would slowly deposit and build up in cold fittings until they were blocked off completely. This was especially an issue in valves and regulators with large pressure drops, as the cooling effect of adiabatic expansion would in some cases bring the gas temperature to below freezing. Heavy tars like naphthalene would then form solid deposits on the control valve stems, causing the valves to stick open or shut. These problems were remedied after several days when all problem areas had been identified and wrapped in heat tape, and tar condensation was not as severe a problem at the end of Test FBG004 or during Test FBG005.

Dolomite was added to every batch of lignite and blended biomass/coal in Test FBG004 at a blend ratio of 20 grams of dolomite per pound of coal. Dolomite is known to capture both CO_2 and H_2S during lignite gasification as well as to help crack tars into gaseous components, and it was added to help improve syngas quality. Although the FBG suffered several system upsets as a

result of plugged lines, the addition of treated biomass to the lignite did not seem to have any adverse effect on operating conditions. Based on the temperature distribution in Figure 6, adding 30% treated switchgrass and treated DDGS to the feed actually seemed to help system performance. Signs of agglomeration were corrected and, as can be seen in Table 5, the temperatures rose when biomass was added to the coal. When switchgrass was mixed with the coal, the coal feed rate set point did have to be raised by 75% to account for the lower density of the switchgrass. The rate was then lowered back to its normal set point when the feed was switched to 30% DDGS and was kept the same when feed was switched to 30% olive pits.

The reactor was eventually taken off-line because of agglomeration. However, because each fuel was run for several hours, it is clear from Test FBG004 that leached biomass can be cogasified with lignite coal without causing significant short-term operational issues. The agglomeration that ultimately stopped the test was the result of a loss in coal feed, which allowed the bed to burn out and become hot enough for ash to melt. Prior to this loss in coal feed, the temperature distribution in the bed was fairly steady, even after the gasifier had been brought back online following a complete shutdown on the night of October 8.

4.1.1.4 Test FBG005

Most of the trouble areas identified in Test FBG004 were heated in Test FBG005 to avoid problems with condensation. However, in some cases, this only created new problems. For instance, the line exiting the recycle syngas surge tank was heated because the large pressure drop out of this tank caused adiabatic expansion and cooling, leading to rapid plugging in Test FBG004. The gasifier was taken off-line in Test FBG005 for several hours to repair an

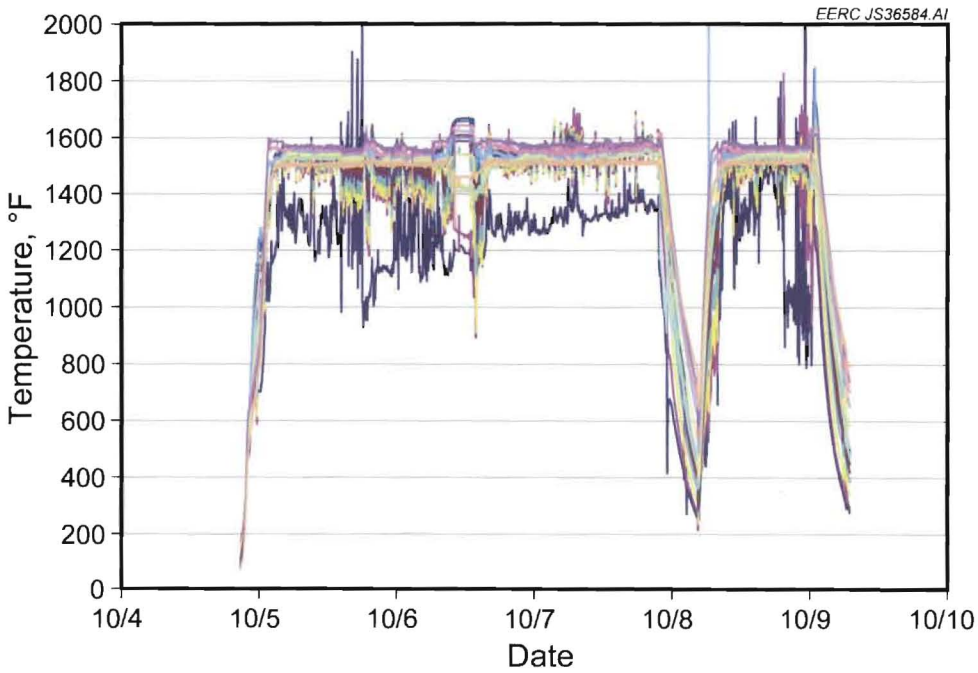

Figure 6. Bed temperature distribution during Test FBG004.

Table 5. Average Run Conditions During Test FBG004

Feed:	100% Lignite	30% Switchgrass 70% Lignite	30% DDGS 70% Lignite	30% Olive Pits 70% Lignite
Bed Temperature, °F	1513	1550	1533	1527
Freeboard Temperature, °F	1547	1558	1555	1557
Feed Rate, lb/hr	8.8	8.4	8.1	8.8
Gas, scfh				
Recycle	581	558	568	584
Steam	365	374	372	397
Nitrogen	27	57	52	0
Oxygen	90	84	84	85
Purge	172	160	150	156
Outlet	136	154	417	72
Bed dP, in. H_2O	29	27	31	31
Freeboard dP, in. H_2O	6.9	10.5	11.7	15.3
Distributor Plate Pressure, psig	438	402	412	441
Bed Pressure, psig	428	394	396	422
Freeboard Pressure, psig	426	391	394	419
Start of Test, dd/mm	10/5/2009	10/7/2009	10/7/2009	10/8/2009
hh:mm	0:58	10:50	16:48	16:37
Test Duration, hh:mm	48:03[1]	5:58	9:39	7:04

[1] An additional 3:49 of lignite run time was conducted following an upset during the 30% DDGS test, but this was not counted as it did not approach steady state.

auger. Less than an hour after the gasifier was restarted, all of the fittings downstream of the surge tank quickly plugged and led to a complete loss in recycle syngas and purge flow. It appears that the gas in the surge tank and exit lines became warm enough to vaporize any condensed tars when gas flow stopped, and these tars were then carried downstream and redeposited on cooler valve stems when flow resumed. The FT reactor suffered from a similar issue, with vaporized tars passing uncondensed through heated lines, as will be shown in Section 4.1.2.4.

Table 6 provides average run conditions for Test FBG005. As with Test FBG004, 20 grams of dolomite per pound of coal was added to every batch of feed to minimize sulfur, tars, and CO_2.

In contrast to the results of Test FBG004, Test FBG005 suggests that the addition of 30% DDGS to lignite had a detrimental effect on gasifier operation. This is probably not a valid result, as the loss of recycle and purge gas occurred only 13 minutes after DDGS was added to the coal, and the system had to be taken off-line for over an hour and a half to clear out the lines. This is seen as a bump in temperatures in Figure 7. When the gasifier was restarted, bed temperatures were steady but not as high as they had been before the shutdown, indicating that some agglomeration may have occurred when the system was down.

When feed was switched to 100% DDGS, problems arose quickly. A primary cause of these problems was that the lower density of the DDGS relative to lignite resulted in a lower

Table 6. Average Run Conditions During Test FBG005

Feed:	Lignite	30% DDGS 70% Lignite	100% DDGS	30% Olive Pits 70% Lignite
Bed Temperature, °F	1490	1459	1457	1459
Freeboard Temperature,°F	1542	1547	1556	1552
Feed Rate, lb/hr	8.7	9.1	7.5	N/A
Gas, scfh				
Recycle	467	375	422	413
Steam	365	408	419	418
Nitrogen	8	4	8	0
Oxygen	52	52	52	55
Purge	179	192	161	236
Outlet	141	135	103	138
Bed dP, in. H_2O	36	62	59	62
Freeboard dP, in. H_2O	13.7	16.6	26.1	22.4
Distributor Plate Pressure, psig	362	361	354	361
Bed Pressure, psig	337	350	342	350
Freeboard Pressure, psig	335	347	337	346
Start of Test, dd/mm	11/30/2009	12/1/2009	12/2/2009	12/2/2009
hh:mm	11:58	22:05	10:30	22:50
Test Duration, hh:mm	25:57	10:58	6:42	2:04

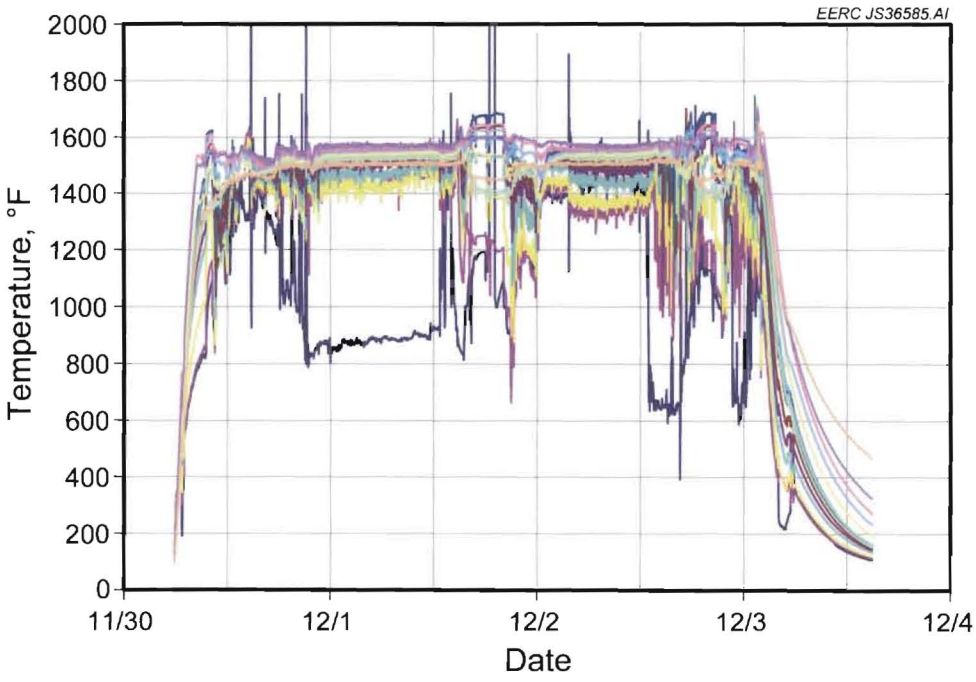

Figure 7. Bed temperature distribution during Test FBG005.

flow rate. Although operators noticed that the flow rate had decreased after nearly 3 hours, by this time, the bed temperatures and CO_2 concentration had risen noticeably. After the feed rate was corrected, the temperature distribution became erratic, indicating that agglomeration had begun to form at the higher O_2:feed ratio and operating temperatures. This agglomeration remained for the duration of the test, mostly obscuring any temperature trends when feeding 30% olive pits in lignite during Test FBG005.

4.1.2 FT Reactor Operation

As expected, the FT process appeared to be feedstock-agnostic, with no change observed in product quality when the gasifier was switched from one fuel to another. However, significant changes in catalyst behavior were observed over time, indicating that the catalyst was beginning to deactivate. Table 7 summarizes the run conditions and primary results for each test.

4.1.2.1 Test FBG002

FT reactor operation was somewhat intermittent during Test FBG002, as this was the first time that the reactor had been operated using online syngas. The FT reactor was taken off-line for several hours and restarted three times during the test period, and the pressure, temperature, and gas flow rates were adjusted several times as operators learned how to achieve the desired conditions. Despite the intermittent and variable operation, the system performed fairly well, achieving the lowest STLG and highest conversion of any test conducted during this project. Although Table 7 captures average data, it is also interesting that CO and H_2 conversion rose significantly during testing from around 20% when the reactor was first started to a stable value of over 70% by the week's end.

Figure 8 shows GC–mass spectroscopy (MS) results for the FT liquids collected in Test FBG002, organized chronologically from top to bottom. Normal paraffin peaks were identified, and all GC peaks between normal paraffins were simply grouped by the next-largest normal paraffin peak to give an approximate product distribution by chain length. This method is not entirely accurate because some compounds will have GC retention times greater than their corresponding normal paraffin, but it does give approximate results and requires significantly less time than manually identifying each GC–MS peak.

One of the more notable features of Figure 8 is the kink on August 27 between 15:00 and 19:30. This kink is due to a gasifier upset that caused a large amount of N_2 to be introduced to the syngas, and the change in syngas composition had a clear effect on product distribution until the nitrogen was bled out of the recycled syngas. A similar effect on product distribution can be seen in the first and last samples analyzed, when neither the gasifier nor the FT reactor were operating at steady state.

Ignoring the first and last sample analyzed and also the kink on August 27 between 15:00 and 19:30, there are three main features to note in Figure 8. First, the product distribution becomes slightly lighter with time. The peak around nonane (9 carbons) grows higher as the test progresses. Second, this trend is more or less gradual with time, indicating that it is not the result of a sudden change in feed. (This is clearer if the kink on August 27 is removed from the graph,

Table 7. Average FT Reactor Run Conditions and Product Properties

Test	FBG002		FBG003		FBG004		FBG005	
	Bed 1		Bed 1		Bed 1	Bed 2	Bed 1	Bed 2
Pressure, psig	260		411		328	328	300	299
Inlet Temperature, °F	387		348		322	331	342	350
Average Bed Temperature, °F	511		504		501	499	499	499
Syngas Flow Rate, scfm	0.87		2.18		0.59	0.57	0.46	0.44
Recycle Product Gas, scfm	4.8		6.3		3.8	3.8	3.2	3.0
Outlet Gas, scfm	0.55		1.52		1.03		0.83	
Closure, %								
Run Time, hh:mm	53:07		65:42		37:52		28:45	
(a)	In	Out	In	Out	In	Out	In	Out
H_2	28.3	13.3	13.8	7.1	14.2	7.4	23.4	13.1
CO	15.9	8.3	8.6	4.3	13.1	9.5	14.5	9.8
CO_2	33.0	45.1	20.5	23.2	42.6	43.7	37.5	42.2
CH_4	5.2	8.8	2.1	3.0	1.2	2.7	3.1	4.9
HC	0	1.0	0	0.42	0.35	0.52	0.77	2.1
H_2O	0.13	0.37	0.06	0.30	0.09	0.20	0.15	0.21
N_2	12.7	17.6	53.9	57.7	27.2	32.3	14.9	21.8
Max. H_2S, ppm *(b)*	0.4	N/A	< 1 *(c)*	N/A	0.9	N/A	0.5	N/A
	CO	H_2	CO	H_2	CO	H_2	CO	H_2
Conversion, %	61	65	54	52	24	50	49	58
STLG *(d)*	17.5		23.7		31.6		28.3	
Liquid Product, lb/hr *(e)*	0.26		0.14		0.094		0.16	
Organic:Aqueous Ratio, lb/lb	0.18		0.097		0.062		0.066	
Aqueous TOC, mg/L *(f)*	7880		7950		16,100		25,500	

Notes: (a) IN = syngas, OUT = FT product gas.
(b) H_2S as measured by Dräger tube when FT reactor first brought online.
(c) Exact Dräger tube value not recorded at time reactor brought online.
(d) Selectivity to light gas.
(e) Represents the total liquid product (both organic and aqueous phases).
(f) Total organic content.

but the revised graph is not shown here in the interest of brevity.) These results show that the catalyst was slowly deactivating (producing less wax and more light products) during Test FBG002. They also show that, although the catalyst was deactivating throughout the week, adding 30% biomass to the gasifier feed did not have any significant impact on FT catalyst behavior or product quality. An initial change in catalyst activity is common and has been observed with this catalyst in laboratory-scale testing.

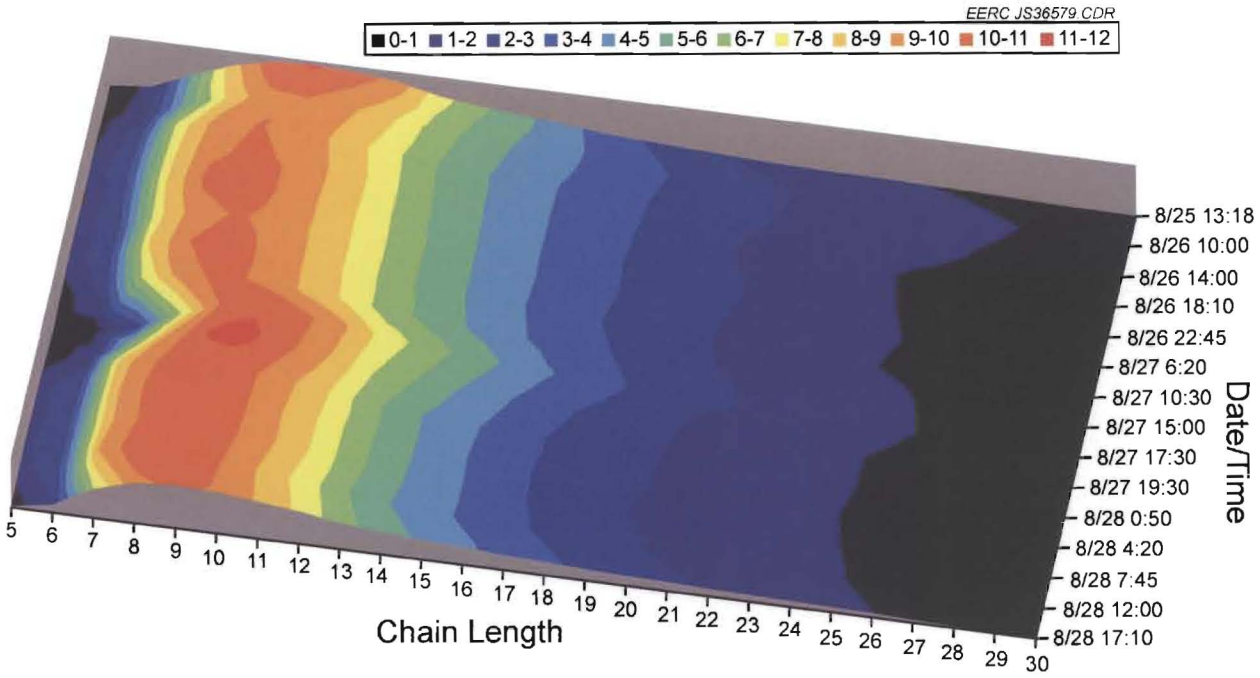

Figure 8. GC–MS results with time for Test FBG002.

4.1.2.2 Test FBG003

In terms of FT reactor operation, the system performed fairly well during Test FBG003, especially considering that the syngas supply rate was restricted by parallel operation of a thermal oxidizer (Section 4.1.1.2). Initially, syngas flow to the FT reactor was intermittent and low (similar to operation throughout most of Test FBG002), but flow was successfully increased from an average of less than 1 scfm to a stable flow rate of more than 2 scfm at 8:30 on September 9. Conversion of CO and H_2 was initially high at 70% prior to this change, but dropped to 50% and remained quite stable thereafter. STLG was steady at 25% after the change was made, as was the organic:aqueous ratio in the FT liquid product, so it is unlikely that the catalyst activity degraded much as a result of the higher flow rate. Because deactivation does not appear to have been significant, the most likely explanation for the sudden drop in conversion when flow rate was increased is simply that the syngas had less residence time on the catalyst surface and thus underwent less reaction on a per-mole basis. Indeed, although the percent conversion of CO and H_2 dropped when the flow rate increased, the liquid production rate more than doubled from 33 to 79 g/hr (0.17 lb/hr) and remained steady for the duration of Test FBG003.

The FT liquid samples from Test FBG003 were either misplaced or accidentally destroyed before they could be analyzed. Likewise, all water samples were combined and destroyed, so no analysis of the FT water by-product could be made. As a result, it is impossible to know for certain what effect the increase in flow rate at 8:30 on September 9 had on product quality. However, the STLG appears to have increased slightly after the change (although this is hard to

ascertain from the graph in Appendix A), and the organic:aqueous ratio in the FT liquid product dropped to less than 0.10 and then held steady. Thus it appears that the higher flow rate resulted in more light gas and less liquid recovery. This finding is reasonable, as FT synthesis is based on chain propagation, and pushing product through the reactor at a faster rate offers less time for hydrocarbon chains to grow and results in poorer selectivity [16]. No discussion has yet been made of the reason for the much lower organic:aqueous ratio in Test FBG003 as compared to Test FBG002. In Test FBG002, all product was collected into an ice-cooled pot to minimize evaporative losses. Operators forgot to pack this pot in ice in all later tests, causing significant loss of light organic material and negatively impacting the organic:aqueous ratio. Further discussion of the loss of organic product is given in the next section.

4.1.2.3 Test FBG004

FT reactor operation was extremely erratic during Test FBG004 because of the lower ambient air temperature, as discussed in Section 4.1.1.3. Tars from the gasifier condensed not only in the exposed gas lines but also in the FT reactor inlet regular and flowmeters, forcing operators to shut down the FT system several times during the week so that these instruments could be removed and cleaned. The FT system was intentionally taken off-line and restarted five times during 4 days of operation, not including times during which inlet flow was lost because of plugging. Heat trace was successfully applied to the FT inlet lines and instruments at 9:00 on October 7, but continued problems with the gasifier itself prevented stable operation until after 14:00 on October 8. As the gasifier was shut down at 23:55 on the same day because of a plug, very little FT steady-state data are available for Test FBG004, and the information in Table 7 represents the weighted average of a wide range of non-steady-state values.

During the brief period of stable operation between 14:00 and 23:55 on October 8, STLG averaged 30%–40% and appeared to be increasing toward 50% before the system was finally shut down. CO and H_2 conversion were both trending downward during this 10-hour period. In previous tests, STLG had not averaged much more than 20%, and CO conversion had more closely matched H_2 conversion and averaged 50% or more. Moreover, STLG and conversion were quite stable over the course of an entire week in previous tests, so it is remarkable to see both values degrading in a 10-hour period in Test FBG004. In addition to the indications of catalyst deactivation given by STLG and conversion, it is also remarkable that water production rate trended strongly upward with time on stream from 17 to 67 g/hr in Test FBG004, while the organic production rate remained fairly constant. In no other tests did water or liquid production rates trend upward over the course of the week.

One major difference between Test FBG004 and previous tests was that both FT beds were utilized with the expectation that the fresh catalyst in the second bed would give better conversion. Because this catalyst bed was never tested on its own, it is impossible to say what effect the fresh catalyst might have had on average system performance.

Assuming that the catalyst in the second bed was no less active than the catalyst in the first bed at the start of testing, the FT catalyst must have undergone significant deactivation before or during Test FBG004, especially considering that deactivation was observed during the 10 brief hours of stable operation on October 8. During this period, temperature, pressure, and flow rates

were similar to those in Test FBG002 (when conversion was over 60% and STLG was around 18%), so the rapid catalyst deactivation does not appear to be the result of operating conditions.

Other than the use of the second reactor bed and the intermittent operation, the only major difference between Tests FBG002 and FBG004 was the syngas composition. H_2 and CO both held fairly constant at 15%–18% during the 10 hours of steady-state operation on October 8. CO_2 in the syngas increased from 40% to 47% during this period, and CO_2 in the recycled product gas increased from 47% to more than 53%. As is clear from Table 7, average syngas CO_2 was higher in Test FBG004 than in any other test. High partial pressure of CO_2 is known to have a detrimental effect on iron-based FT catalysts and is the most reasonable explanation for the increased STLG observed in Test FBG004 [18]. The low and nearly identical levels of both CO and H_2 explain why conversion was not as expected, as the H_2:CO ratio was closer to 2:1 in Tests FBG002 and FBG003. Under ideal conditions, iron-based catalysts would catalyze the water–gas shift reaction to convert water by-product into excess H_2, and a H_2:CO ratio of 1:1 would result in equal conversion of both components. However, high partial pressure of CO_2 inhibits the water–gas shift reaction and allows excess water to oxidize and deactivate the catalyst. As a result, CO conversion was much lower than H_2 in this test, and both STLG and conversion decreased over time as CO_2 concentration in the product gas increased.

One odd feature that is immediately apparent when comparing Figures 8 and 9 is the loss of most of the product lighter than nonane (C9), causing the main peak to shift toward the heavier range in Test FBG004. This observation completely contradicts every other trend discussed so far, as it would suggest that STLG was lower and that the catalyst was more active at producing waxes in Test FBG004 than in Test FBG002. The most likely explanation for the loss of light material is that product was collected into an ice-cooled pot during Test FBG002 but

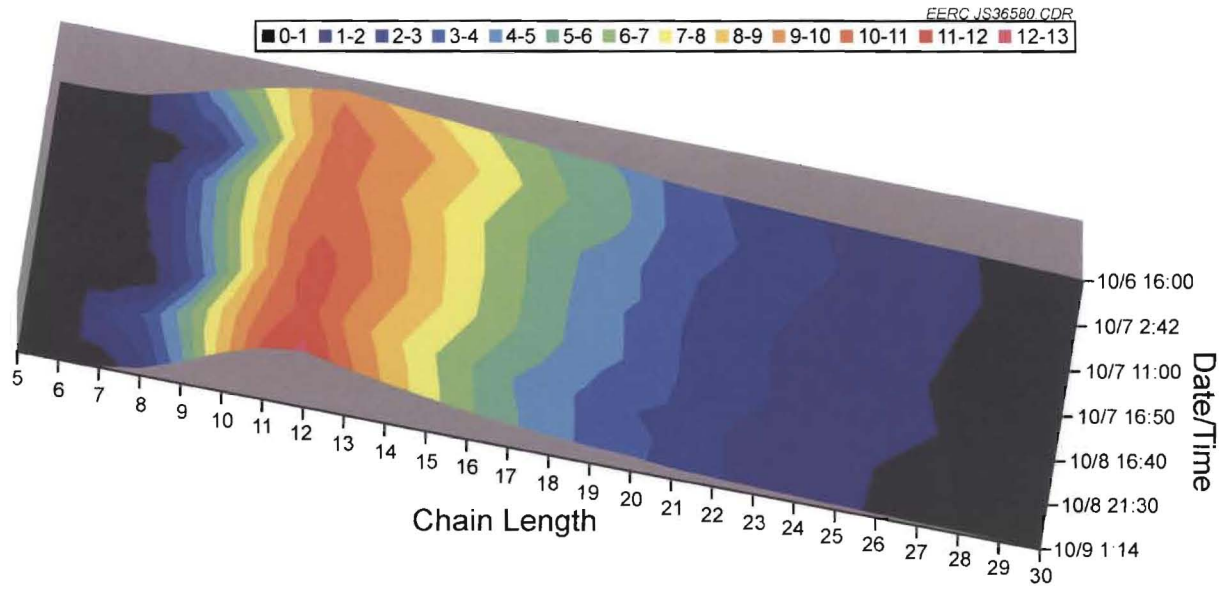

Figure 9. GC–MS results with time for Test FBG004.

was collected at room temperature thereafter. In later tests, the higher temperature in the pot, which is held at a slight vacuum, probably allowed more of the light product to vaporize before it could be recovered as liquid. For this reason, the organic:aqueous ratio for Test FBG002, shown in Table 7, cannot be compared to the organic:aqueous ratio for any later tests, as more of the organic liquid was almost certainly lost.

Ignoring the loss of material lighter than nonane, the GC–MS trend for Test FBG004 shows a change in product quality over time, with less wax formation and more light product formation. This explains the increasing rate of water production mentioned previously, as more water is generated when producing light FT products than when producing heavier hydrocarbons. The trend is fairly continuous over time and does not occur in a discrete step, indicating that it is a result of general process conditions rather than of changing gasifier feed from coal to biomass. Although some increase in light product formation was observed in Test FBG002, the rate of change is much more pronounced in Test FBG004, indicating a greater degree of catalyst deactivation over time than observed in earlier testing. The likely reason is poor syngas quality, as discussed previously. Not only was the syngas quality generally poor, but prior to the steady-state period on October 8, the FT reactor itself was often idling hot with only recycle product gas flow because of losses in syngas flow. Recycling the product gas without introducing fresh syngas caused CO_2 to concentrate in the FT product gas, and this probably caused the catalyst to deactivate at an advanced rate.

4.1.2.4 Test FBG005

Although the FT reactor was taken off-line for around 13 hours during Test FBG005 because of a gasifier upset, the system was much more stable than in Test FBG004, as heat trace was used to prevent tar and water condensation in exposed lines and fittings. Flow was still somewhat intermittent because of the cold weather (Figure 5), but overall, operation was fairly stable.

Prior to Test FBG005, CO was passed over both FT catalyst beds in the hope of regenerating oxidized catalyst. This was the method used to dry and calcine the catalyst when it was first loaded prior to Test FBG002. As had been observed in the initial activation, CO_2 was evolved as oxygen was driven from the catalyst surface. CO flow was maintained as before until the CO_2 concentration dropped to around 1%, indicating that most of the oxygen had been removed.

As shown in Table 7, syngas and recycle flow rates were kept lower during Test FBG005 than in any earlier test. The syngas composition was relatively similar to that of Test FBG002, with less than 40% CO_2 during most of the test and a H_2:CO ratio of 1.6:1. The quality was substantially better than in Test FBG003, when the syngas had more than 50% nitrogen dilution, H_2 exceeded 15% for only 2 hours, and CO never exceeded 10%. All of these factors suggested that catalyst performance should have been better than in Test FBG003 and nearly as good as in Test FBG002.

However, CO conversion averaged only 49% and H_2 conversion 58%, which was similar to Test FBG003 despite the higher concentration of reactants and the longer residence times.

STLG was worse than in Test FBG002 or Test FBG003, and the organic:aqueous ratio was not significantly different than in Test FBG004. These facts all demonstrate that the attempt to regenerate catalyst under CO was largely unsuccessful.

Figure 10 confirms that the FT product was not greatly improved by catalyst reduction under CO. As with Tests FBG003 and FBG004, product was collected at room temperature in Test FBG005, so most light product was vaporized. The product from Test FBG005 does not appear to be as consistent as the product from previous tests. However, much of this is due to the presence of aromatics in the FT liquids, as seen in Figure 11 for the December 2 16:00 sample. In earlier tests, the lines to the FT reactor were not heated, and any aromatic-rich tars that escaped from the gasifier quench pots were condensed before reaching the FT system. After the poor system operation observed in Test FBG004 as a result of cold weather, the inlet lines were wrapped in heat tape. This prevented the inlet regulator and rotameters from becoming plugged, but it also allowed tars escaping from the gasifier quench system to remain in a vapor state and reach the FT reactor with the syngas. The benzene peak at C7 in Figure 11 is minor or nonexistent in most other samples analyzed, and benzene is not a typical FT product, indicating that it is probably contamination from the gasifier. (It should be noted that benzene is a C6 molecule, not a C7 molecule. As explained in Section 4.1.2.1, all GC–MS peaks except normal paraffins are grouped with the next largest normal paraffin peak in the GC–MS response. Benzene appears between hexane and heptane, so it is counted as a C7 molecule).

Except for samples apparently contaminated with gasification tars, the major peaks in Figure 10 show a fairly strong similarity to those in Figure 9. The TOC of the aqueous phase is also quite large at 25,500 mg/L, which is higher than the bulk average for Test FBG004 but may represent TOC at the conclusion of Test FBG004, when catalyst was fairly degraded. Along with the conversion, STLG, and organic:aqueous ratio, these similarities in the liquid products further

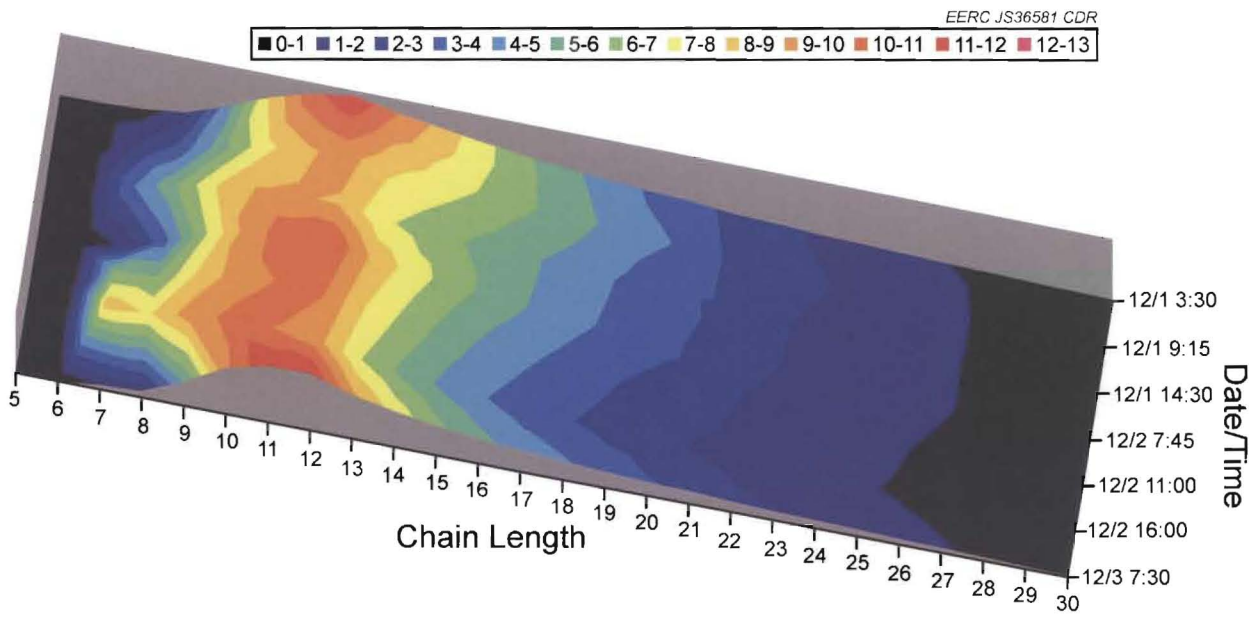

Figure 10. GC–MS results with time for Test FBG005.

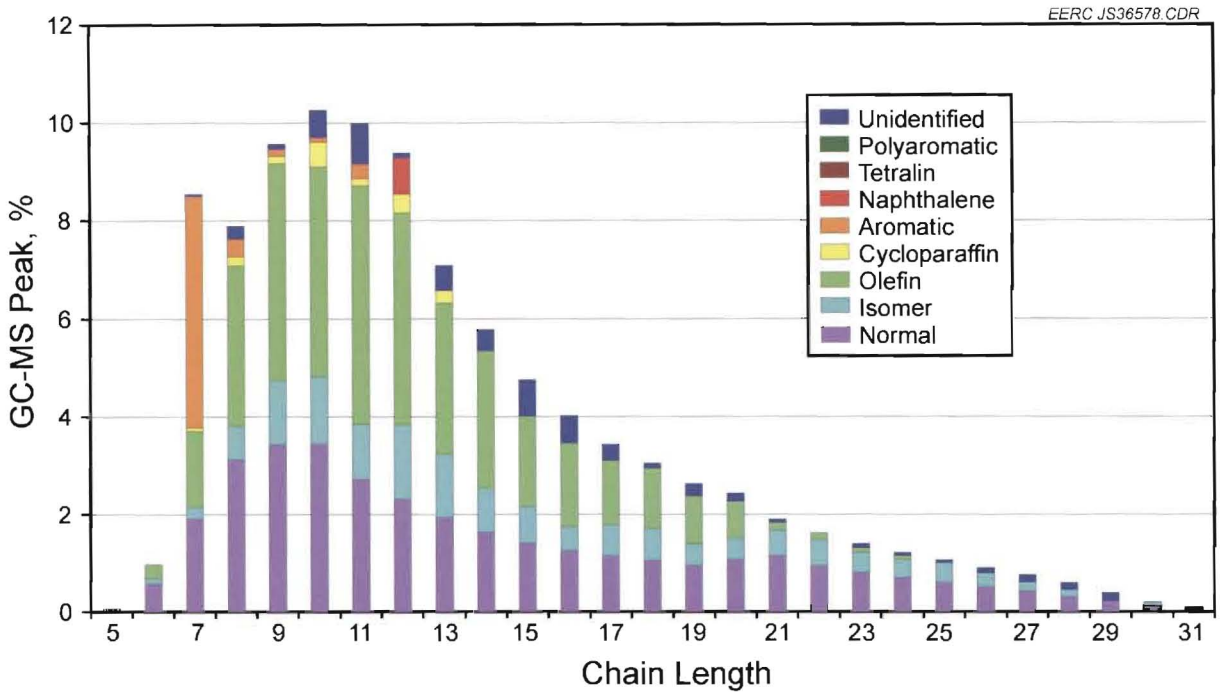

Figure 11. GC–MS peak breakdown for December 2 16:00 sample.

indicate that the attempt to regenerate catalyst between tests was unsuccessful. Because CO_2 was evolved during the regeneration attempt, it is clear that the catalyst had been oxidized, and it is likewise clear that passing hot CO over the catalyst helped to reduce the catalyst. Since the catalyst activity did not recover, it is probable that catalyst deactivation was due to more than simple oxidation.

One possible explanation is coking. Tars from the gasifier were dramatically present in the product from Test FBG005, but lower concentrations of aromatic and cycloparaffinic compounds were also observed in the FT product from earlier tests. The presence of tars on the catalyst surface could lead to deactivation by coking [15]. Another possible explanation for catalyst deactivation is catalyst sintering. As the active sites on the catalyst surface sinter together, they lose surface area, and the catalyst becomes less active [15]. Both coking and sintering of iron-based FT catalysts could be partially undone by fully oxidizing the catalyst under dilute air before reducing under CO. Although this method was not attempted in this project, it may have helped to recover catalyst activity and should be examined in future testing of iron-based FT catalysts.

One other possible candidate for catalyst deactivation is sulfur poisoning. Sulfur poisoning is known to deactivate iron-based FT catalysts, but there is good reason to believe that sulfur poisoning was not significant in this project. The FT reactor uses a packed-bed design, so sulfur would tend to be captured in the top of the beds and would not have a noticeable impact on catalyst performance until sulfur poisoning had reached a significant bed depth. Because H_2S was kept to less than 1 ppmv (being detected only at the ppb range by GC–PFPD) during all

testing, it does not seem likely that sulfidation should have penetrated deep into the beds by the third week of testing, especially given that the second bed contained fresh catalyst.

4.2 Task 2 – Catalytic Development and Production

Because the catalyst generated under Task 2 was produced too late in the project to be used for FT synthesis in this project, no discussion can be undertaken regarding the FT activity of the catalyst formulation developed under this work.

4.3 Task 3 – Process Simulation and Product Enhancement

4.3.1 Process Simulation

Empirical inputs for the AspenPlus-based model were selected using data from Test FBG002 (Section 4.1.1.1). Table 8 compares the measured gas concentration to the concentration in the model. It should be noted that measured syngas concentrations are as-reported in this table and do not total 100%. The components in the gas stream were predicted reasonably well by the model. Some discrepancies arise where the equilibrium predictions from the model do not match with the experimental data, and N_2 may be overpredicted because the purge rate measured at the gasifier does not accurately reflect the amount of nitrogen entering the system. Overall, however, the syngas predictions are fairly close. It should also be noted that some error could lie in the LGA measurements.

Figure 12 shows the liquid hydrocarbon distribution as measured from the FT reactor and compares it to the model predictions. The GC–MS data shown in Figure 12 are from 22:45 on August 26 and were carefully scrutinized to give a more accurate product distribution than those shown in Section 4.1.2. (This level of scrutiny was not applied to all samples because of the significant amount of time required to manually identify all peaks.) Although the model predicts the approximate shapes of the normal and olefin distributions reasonably well, the relative ratios of normal paraffins to olefins are incorrect, particularly for molecules with 10 or fewer carbon

Table 8. Exit Gas Concentrations: Gasifier Data vs. Model Predictions

Component (dry basis)	Syngas Concentration, mol%	Model Prediction, mol%
H_2	28.3	29.6
CO	15.9	15.5
CO_2	33.0	36.6
CH_4	5.2	4.16
HC	0.00	0.00
H_2O	0.13	0.13
N_2	12.7	14.0
H_2S	<1 ppm	0.30 ppm

H_2S is postcapture as measured by Dräger tube.

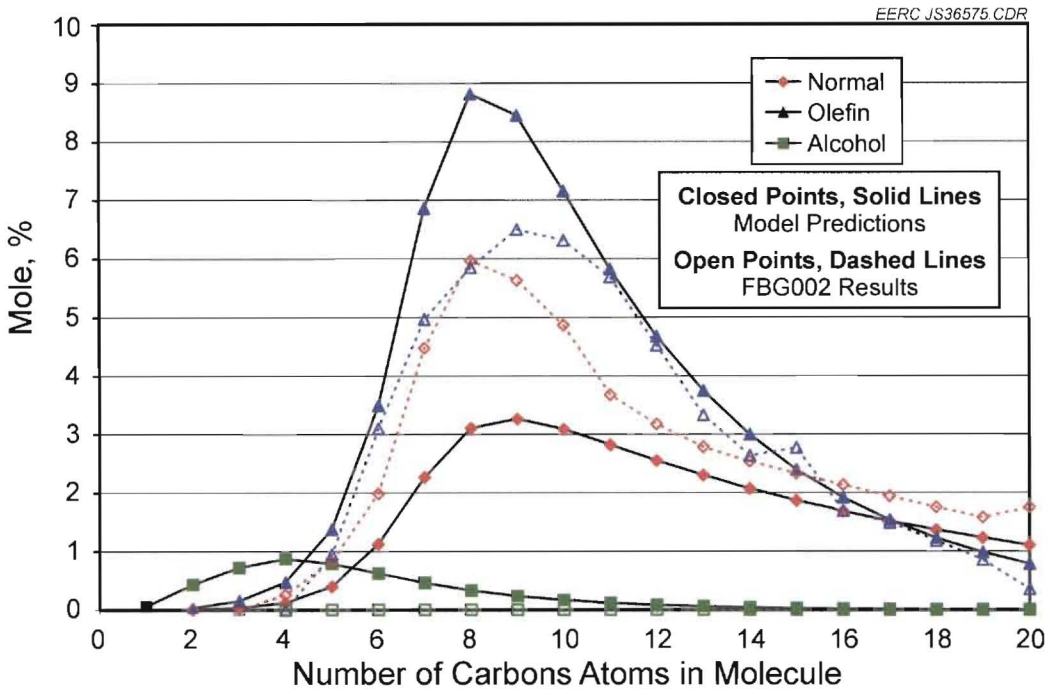

Figure 12. Liquid hydrocarbon distribution: reactor data vs. model predictions.

atoms. Also, no alcohols could be positively identified in the organic phase of the FT product despite the obvious presence of alcohols in the aqueous phase as detected by GC-flame ionization detection (FID).

There are at least two likely causes for these discrepancies. First, the α-values for the ASF model were based on laboratory data generated from gas with a H_2:CO ratio of 1:1, while the bench-scale data were generated from syngas with a H_2:CO ratio of 1.8:1. Given the higher ratio, more light compounds would be expected, as would some degree of product saturation (i.e., fewer alcohols and olefins) [16]. Lighter alcohols are more easily solubilized in water than are heavy alcohols, so the higher H_2:CO ratio was not only likely to produce less alcohol, it also produced alcohols that were more likely to escape to the aqueous phase. As seen in Table 7, the tests with the highest STLG also had the highest aqueous TOC. GC–FID analysis of the aqueous phases verified that the high TOC values were due almost entirely to light alcohols.

A second cause for the discrepancies in Figure 12 are flaws in the bench-scale data. It is clear from GC–MS analysis of the bench-scale FT product that many of the olefins were isomerized, something that was not observed in FT liquids collected from the laboratory reactor. This isomerization resulted in a large number of very small olefin peaks, which are more difficult for the GC–MS to correctly identify than are large, unbranched olefin peaks. Because many of the isomerized olefin peaks were probably not identified, less olefin was likely measured than was actually present. Similarly, there are several GC–MS peaks that may represent alcohols in the organic phase, but the signal quality is far too poor to be certain. GC–FID analysis of the aqueous phase revealed that the alcohols, like the olefins, had been isomerized. As the already dilute primary alcohol peaks were broken into even more dilute and harder-to-detect secondary

and branched alcohol peaks, it is not surprising that the GC–MS failed to correctly identify any of these alcohols in the organic phase.

4.3.2 Product Enhancement

Most of the results and analysis from product enhancement cannot be discussed in this report at the request of the catalyst supplier. However, it can be stated that single-pass isomerization was unexpectedly poor. The cause for this was a failure to follow a standard procedure for hydrotreating, and as such, the issue has been identified and can be easily corrected.

Because of the poor isomerization, the FT product was recycled through the hydrotreating reactor several times to increase isomerization to a level of 68%, which is still fairly low based on previous EERC experience. A small amount of FT product is lost during each pass through the reactor to sampling, residue, and cracking, and so any further hydrotreating was considered prohibitive given the small sample size. The hydrotreated FT product was then distilled to yield a jet cut, but this product had a freeze point of -45°C as compared to the JP-8 specification of -47°C or lower. The density was also slightly low, but this is typical of FT products and is not an issue if the product is blended with petroleum-derived jet fuel.

Several additional attempts were made to redistill a specification-compliant jet fuel, but because of the small sample size and the loss to residue with each additional distillation, this effort was abandoned. As a result, a specification-compliant synthetic jet fuel was never produced, nor is it clear that additional distillation would have been helpful given the low level of isomerization. Although no products from the EERC's packed-bed FT reactor were fully upgraded to jet fuel in this project, the product enhancement effort did demonstrate that the concept is feasible and has identified several issues that will need to be considered if small-scale, distributed FT systems are utilized in the future.

5.0 SUMMARY

A high-pressure FBG was successfully operated on a variety of coals and biomass types, including North Dakota lignite and two potential North Dakota biomass resources. Biomass pretreatment by leaching helped to prevent ash agglomeration, and biomass torrefaction led to higher gasification temperatures. Heating various fittings and valves was necessary when ambient temperatures dropped, as the colder temperatures led to plugging of exposed lines by condensed tars. This solution may not be feasible for sustained, long-term operation of small-scale distributed gasification and FT technologies. For a small gasifier with minimal auxiliary systems to be operated continuously for a long duration, the system design will need to either avoid tar production or ensure adequate tar and water removal.

Cogasification of 30% biomass with coal did not appear to create any operating difficulties in short-term operation so long as the biomass was pretreated by leaching. Cofeeding 30% untreated biomass with PRB coal did cause agglomeration, showing that the leaching method was effective at preventing agglomeration. No conclusions can be drawn on the agglomerating

potential for gasifying 100% treated biomass, as the bed had already begun to agglomerate prior to any test in which 100% biomass was fed.

Syngas from the gasifier was successfully treated online to remove sulfur and most moisture and tars and then passed to a packed-bed FT system. The packed beds achieved sustained FT synthesis and temperature control, demonstrating the feasibility of this design for small-scale operation. However, catalyst deactivation was apparent during the 4 weeks of testing. The primary cause of deactivation appears to have been oxidation resulting from high CO_2 concentrations. Gasification tars may also have contributed to catalyst deactivation by coking. For a packed-bed FT system to function long-term in commercial operation, one or more of three solutions will be required: A higher-temperature gasifier design that would allow less tar and CO_2 to be generated on the front end, a CO_2-tolerant FT catalyst such as cobalt, or some method of removing CO_2. High-temperature gasifiers exist but may not be scalable or suitable for low-energy feeds such as lignite and biomass. CO_2-tolerant cobalt-based FT catalysts also exist, and attention should be given to optimizing these for syngas generated from a small-scale gasifier utilizing low-energy feeds. CO_2 as well as other contaminants can be reliably removed from syngas by cooling to subzero temperatures in a solvent such as Rectisol, but this option is not suitable for small-scale distributed operation because of process cost and complexity. If distributed gasification systems are to succeed with iron-based catalysts, focus on high-temperature CO_2 sorbents will be required.

A process for generating kilogram-scale quantities of pelletized iron-based catalyst was conceived of, constructed, and tested in this project. Although the catalyst generated by this process was produced too late to be used for testing in the packed-bed FT reactor, the EERC has demonstrated a process for generating large quantities of uniform pelletized catalyst in a single batch using mostly off-the-shelf equipment.

A model was developed using Aspen Plus that is capable of predicting the gas composition from the FBG and the hydrocarbon distribution from the FT reactor. Although it does not accurately account for the effects of syngas composition on FT product, it has demonstrated a capability to model gasification and relative flow rates of products, and it will continue to be improved by the EERC under upcoming projects. The model may be useful to the North Dakota Industrial Commission in future FT projects, and it will be useful for attracting gasification and FT research dollars to the EERC and by extension to the state of North Dakota.

Product enhancement did not result in a fully compliant jet fuel sample. The effort identified several key issues with upgrading liquids from small-scale packed-bed FT reactors that could be coupled to distributed coal and biomass gasification systems. For these FT liquids to be upgraded continuously, consideration will have to be given to ensuring that proper protocols are followed prior to and during hydrotreating of FT liquids. Although the particular protocols cannot be discussed here, they are fairly easy to perform and are part of a standard operating procedure used during hydrotreating.

6.0 REFERENCES

1. Abrini, J.; Naveau, H.; Nyns, E.J. Clostridium autoethanogenum, sp. nov., an Anaerobic Bacterium that Produces Ethanol from Carbon Monoxide. *Arch. Microbiol.* **1994**, *161*, 345–351.

2. Niederschulte, M. INEOS BioEnergy Process: A Clean, Sustainable Technology for Energy Independence. Presented at Biomass 2009: Fueling Our Future, National Harbor, MD, March 17–18, 2009.

3. Zheng, Y.; Li, L.Z.; Xian, M.; Ma, Y.J.; Yang, J.M.; Xu, X.; He, D.Z. Problems with the Microbial Production of Butanol. *J. Ind. Microbiol. Biotechnol.* **2009**, *36*, 1127–1138.

4. Probstein, R.F.; Hicks, R.E. *Synthetic Fuels*; Dover Publications, Inc.: Mineola, NY, 1982.

5. Skoulou, V.; Kantarelis, E.; Arvelakis, S.; Yang, W.; Zabaniotou, A. Effect of Biomass Leaching on H_2 Production, Ash, and Tar Behavior During High-Temperature Steam Gasification (HTSG) Process. *Int. J. Hydrogen Energy* **2009**, *34*, 5666–5673.

6. Arvelakis, S.; Hurley, J.; Folkedahl, B.; Koukios, E.G.; Spliethoff, H. Fluidized-Bed Gasification of High-Alkali and Chlorine Biomass: Effect of Pretreatments on the Agglomeration Behaviour. In *Proceedings of the International Technical Conference on Coal Utilization & Fuel Systems*; Coal Technology Association, 2008; pp 591–601.

7. Nguyen, M.H.; Prince, R.G.H. A Simple Rule for Bioenergy Conversion Plant Size Optimisation: Bioethanol from Sugar Cane and Sweet Sorghum. *Biomass Bioenergy* **1996**, *10*, 361–365.

8. Börjesson, P.I.I. Energy Analysis of Biomass Production and Transportation. *Biomass Bioenergy* **1996**, *11*, 305–318.

9. Li, L.; King, D.L.; Liu, J.; Zhu, K.; Wang, Y. Metal-Based Adsorbents for Regenerable Deep Desulfurization of Warm Syngas. In *Proceedings – 25th Annual International Pittsburgh Coal Conference*; 2008.

10. Schmidt, R.; Cross, J.; Tsang, A.; Sughrue, E.; Kornosky, R. Sulfur Removal from E-Gas Gas Streams with S Zorb Sulfur Removal Technology (SRT). In *Proceedings – 23rd Annual International Pittsburgh Coal Conference*; 2006.

11. Faaij, A.; van Doorn, J.; Curvers, T.; Waldheim, L.; Olsson, E.; van Wijk, A.; Daey-Ouwens, C. Characteristics and Availability of Biomass Waste and Residues in the Netherlands for Gasification. *Biomass Bioenergy* **1997**, *12*, 225–240.

12. Arvelakis, S.; Gehermann, H.; Beckmann, M.; Koukios, E.G. Agglomeration Problems During Fluidized-Bed Gasification of Olive Oil Residue: Evaluation of Fractionation and Leaching as Pretreatments. *Fuel* **2003**, *82*, 1261–1270.

13. Arvelakis, S.; Koukios, E.G. Physicochemical Upgrading of Agroresidues as Feedstocks for Energy Production via Thermochemical Conversion Methods. *Biomass Bioenergy* **2002**, *22*, 331–348.

14. Svoboda, K.; Pohořelý, M.; Hartman, M.; Martinec, J. Pretreatment and Feeding of Biomass for Pressurized Entrained Flow Gasification. *Fuel Process. Technol.* **2009**, *90*, 629-635.

15. Bartholomew, C.H.; Farrauto, R.J. *Fundamentals of Industrial Catalytic Processes;* John Wiley & Sons, 2006.

16. Davis, B.H. Fischer–Tropsch Synthesis: Relationship Between Iron Catalyst Composition and Process Variables. *Catal. Today* **2003**, *84*, 83–98.

17. Jones, M.; Stanislowski, J.J.; Benson, S.A.; Laumb, J.D. Gasification of Lignites to Produce Liquid Fuels, Hydrogen, and Power. Presented at the 24th Annual Pittsburgh Coal Conference, Johannesburg, South Africa, Sept 10–15, 2007.

18. Ning, W.; Koizumi, N.; Yamada, M. Researching Fe Catalyst Suitable for CO_2-Containing Syngas for Fischer–Tropsch Synthesis. *Energy Fuels* **2009**, *23*, 4696–4700.

EERC
Energy & Environmental Research Center

APPENDIX A

RAW DATA

Printed on Recycled Paper

RAW DATA

The following raw data are provided in chart form for each test. For the gasifier itself:

- Average bed and freeboard temperatures. This allows the reader to see overall trends not readily visible from the individual temperature readouts shown in the main report.
- Flow rates into and out of the gasifier.
- Pressure drops across the fluid bed and freeboard. These indicate bed height (i.e., amount of solids inventory in each section).
- Gasifier pressures.
- Syngas composition as measured by laser gas analyzer (LGA) (It should be noted that in Test FBG002, H_2O was measured in place of O_2 as the LGA had not yet been modified).

For the Fischer–Tropsch (FT) reactor:

- Product gas composition exiting the FT reactor as measured by LGA.
- Flow rates into and out of the FT reactor bed(s).
  - FI901 – Flow rate into FT Bed 1.
  - FI901 – Flow rate into FT Bed 2.
  - FI903 – Flow rate of recycled FT wax into FT Bed 1 (not used).
  - FI904 – Flow rate of recycled FT wax into FT Bed 2 (not used).
  - FI905 – Flow rate of recycled product gas into FT Bed 1.
  - FI906 – Flow rate of recycled product gas into FT Bed 2.
  - Flowrate – Exhaust gas flow out of FT reactor system.
- Pressure drops across FT reactor.
  - DPT901 – Pressure drop across FT Bed 1.
  - DPT902 – Pressure drop across FT Bed 2.
  - DPT903 – Pressure drop across wax trap (unreliable).
  - DPT904 – Pressure difference between dry gas meter and atmosphere (would indicate plugged outlet line).
- FT reactor pressures.
  - PT900 – Pressure downstream of syngas regulator.
  - PT901 – Pressure at top of FT Bed 1.
  - PT902 – Pressure at top of FT Bed 2.
  - PT903 – Quench pot pressure.
- FT reactor temperatures.

- Conversion of CO and H_2.
- Selectivity to light gas.

FBG002
Gasifier Trends

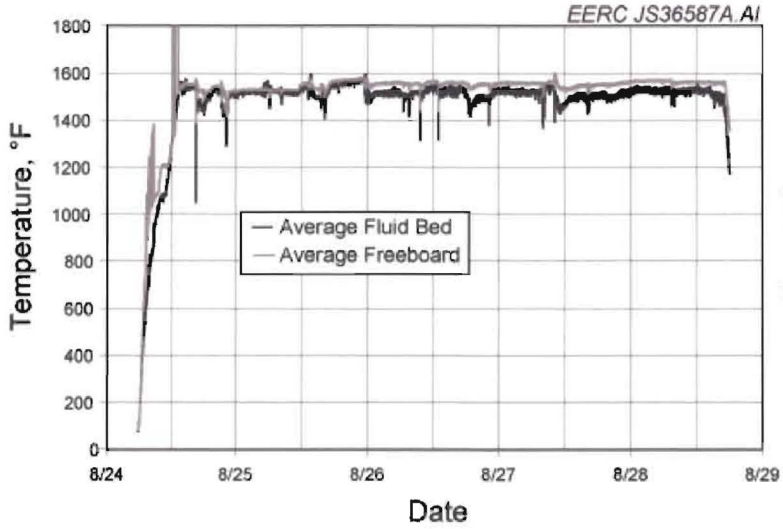

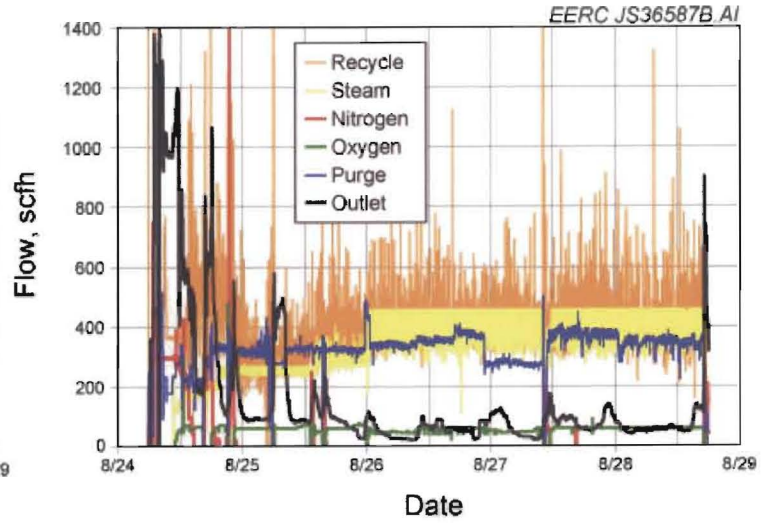

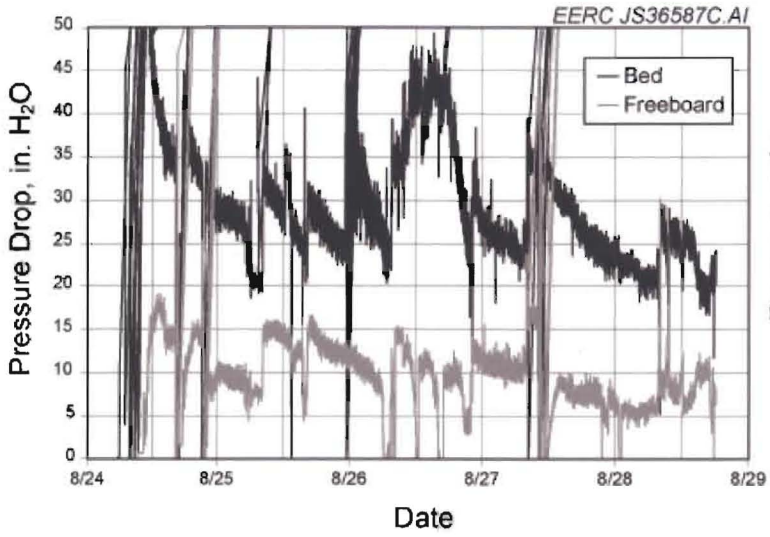

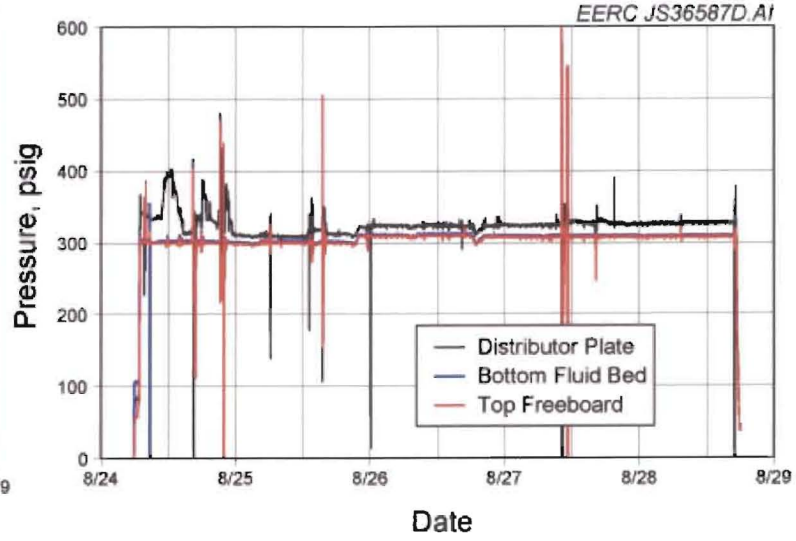

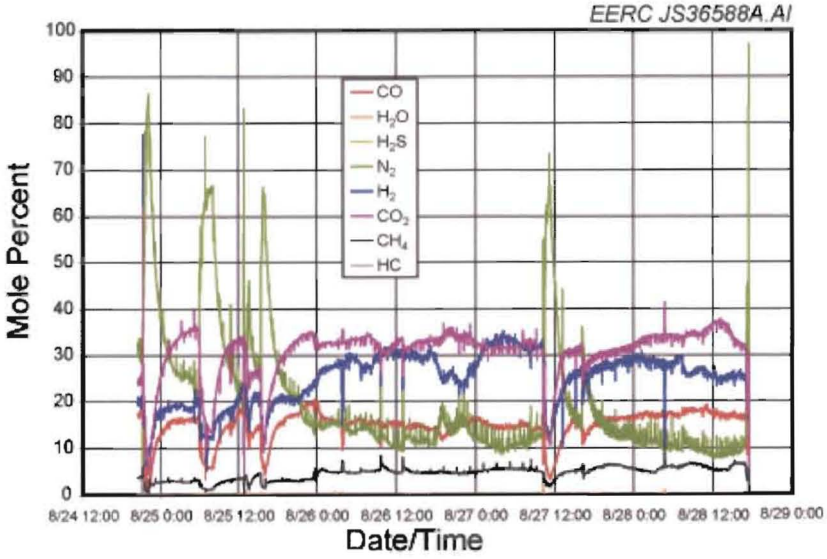

FT Reactor Trends

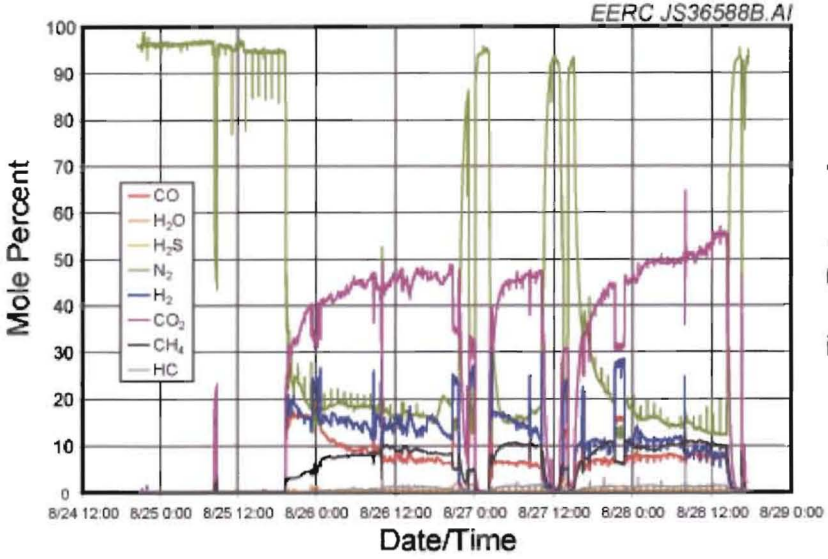

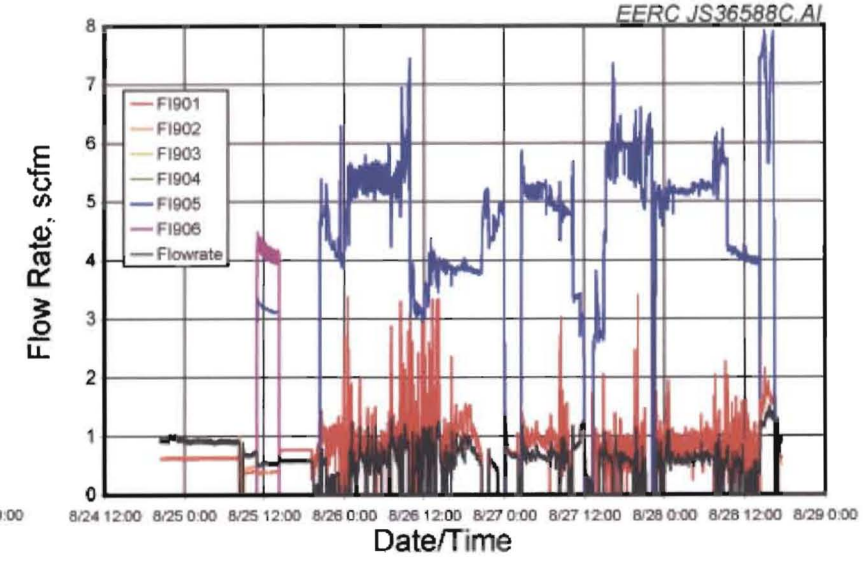

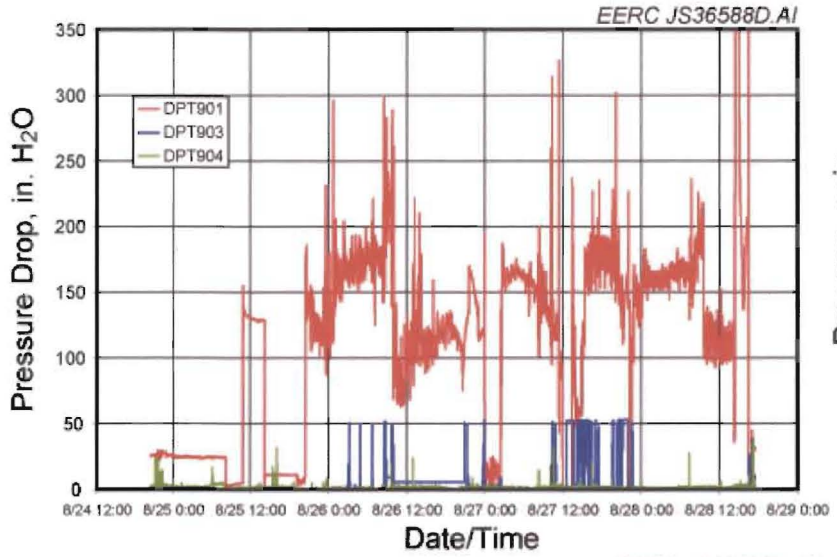
EERC JS36588D.AI
Pressure Drop, in. H2O
DPT901
DPT903
DPT904
350
300
250
200
150
100
50
0
8/24 12:00 8/25 0:00 8/25 12:00 8/26 0:00 8/26 12:00 8/27 0:00 8/27 12:00 8/28 0:00 8/28 12:00 8/29 0:00
Date/Time

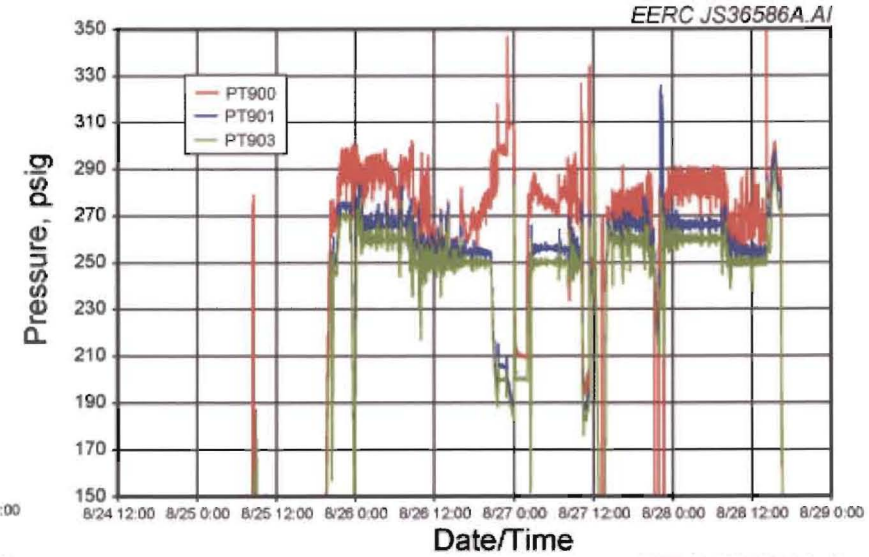
EERC JS36586A.AI
Pressure, psig
PT900
PT901
PT903
350
330
310
290
270
250
230
210
190
170
150
8/24 12:00 8/25 0:00 8/25 12:00 8/26 0:00 8/26 12:00 8/27 0:00 8/27 12:00 8/28 0:00 8/28 12:00 8/29 0:00
Date/Time

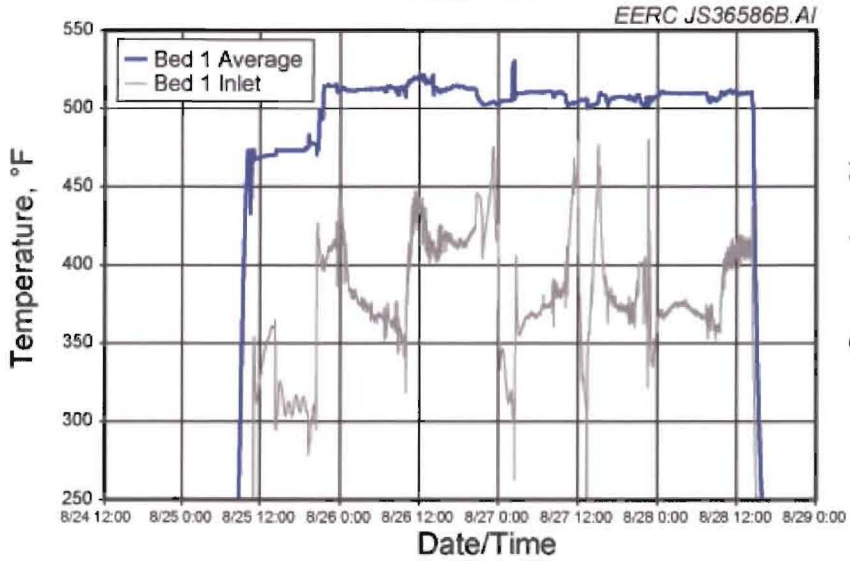
EERC JS36586B.AI
Temperature, °F
Bed 1 Average
Bed 1 Inlet
550
500
450
400
350
300
250
8/24 12:00 8/25 0:00 8/25 12:00 8/26 0:00 8/26 12:00 8/27 0:00 8/27 12:00 8/28 0:00 8/28 12:00 8/29 0:00
Date/Time

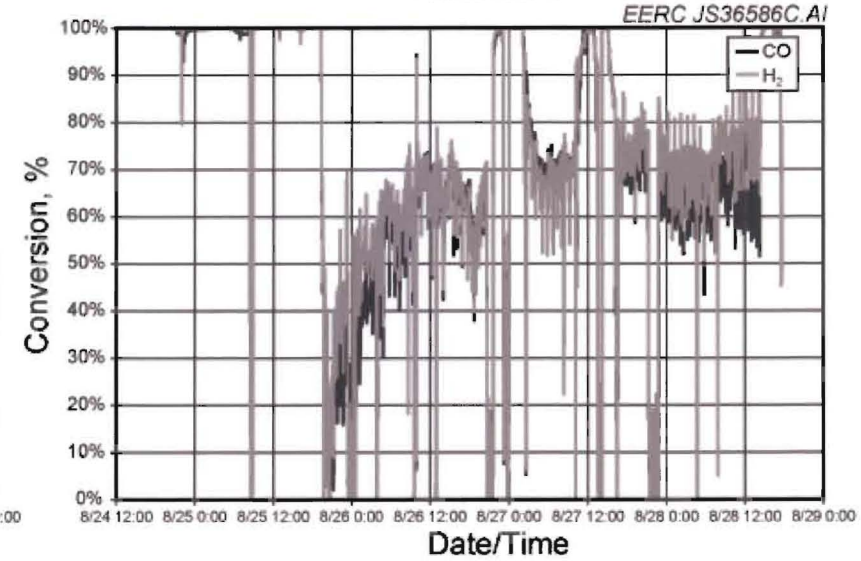
EERC JS36586C.AI
Conversion, %
CO
H2
100%
90%
80%
70%
60%
50%
40%
30%
20%
10%
0%
8/24 12:00 8/25 0:00 8/25 12:00 8/26 0:00 8/26 12:00 8/27 0:00 8/27 12:00 8/28 0:00 8/28 12:00 8/29 0:00
Date/Time

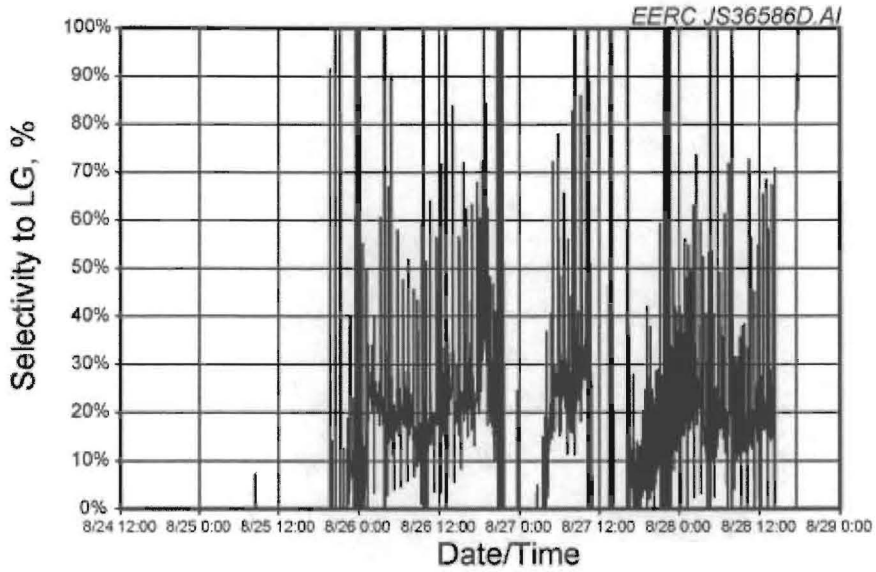
EERC JS36586D.AI
Selectivity to LG, %
100%
90%
80%
70%
60%
50%
40%
30%
20%
10%
0%
8/24 12:00
8/25 0:00
8/25 12:00
8/26 0:00
8/26 12:00
8/27 0:00
8/27 12:00
8/28 0:00
8/28 12:00
8/29 0:00
Date/Time

FBG003

Gasifier Trends

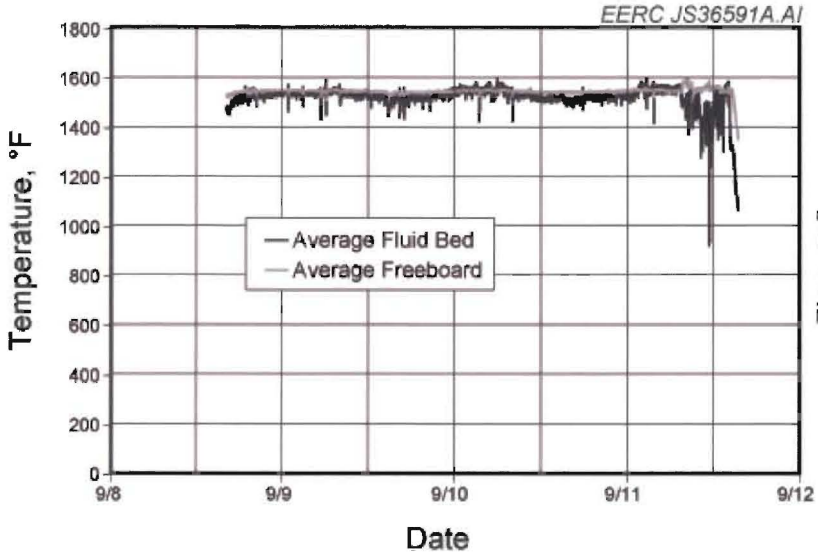

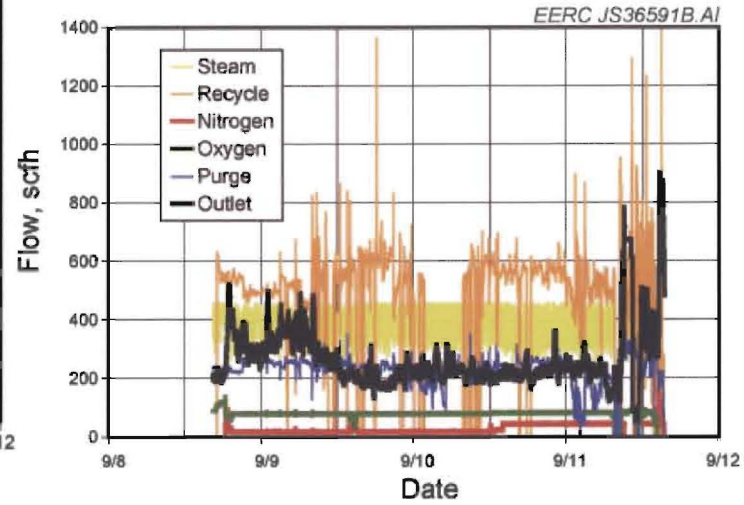

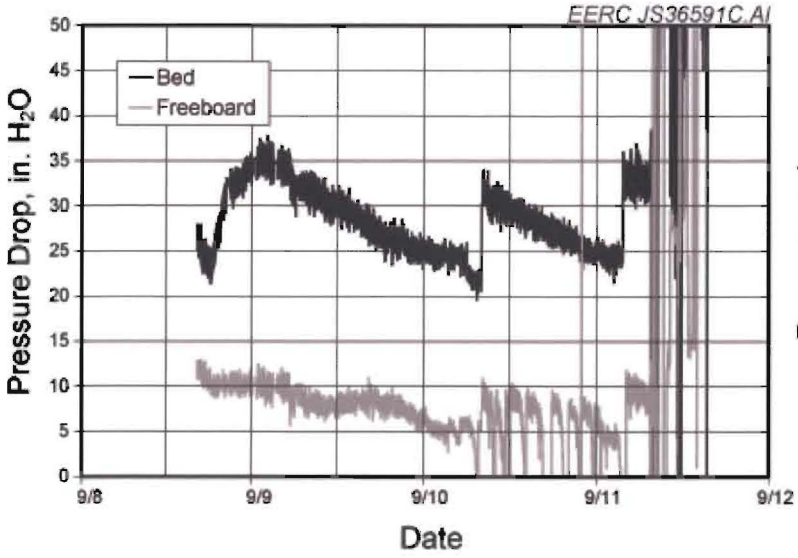

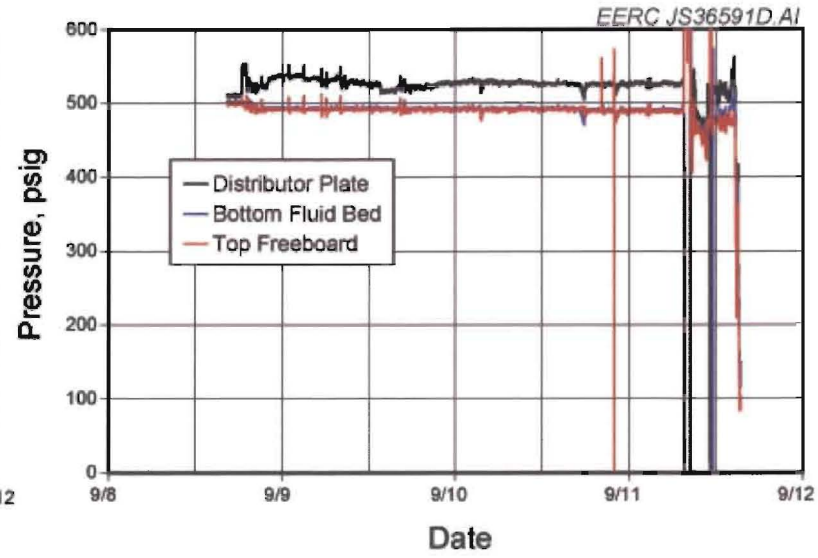

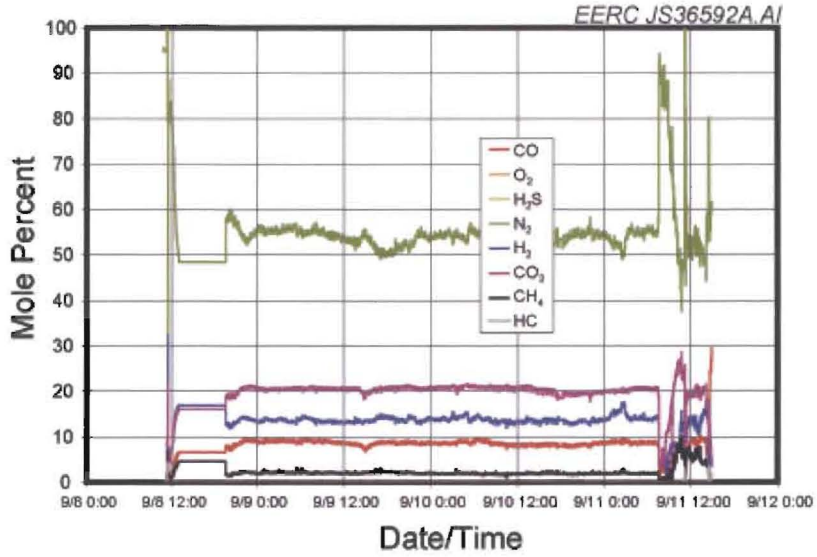

FT Reactor Trends

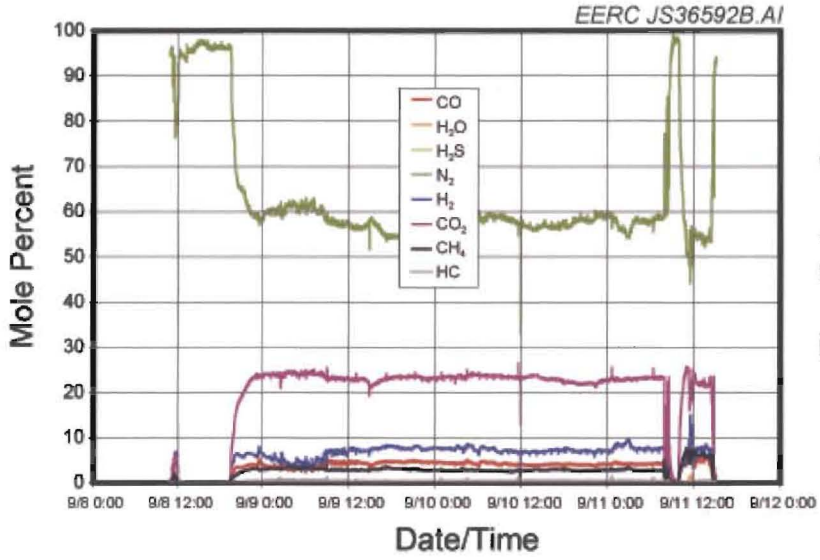

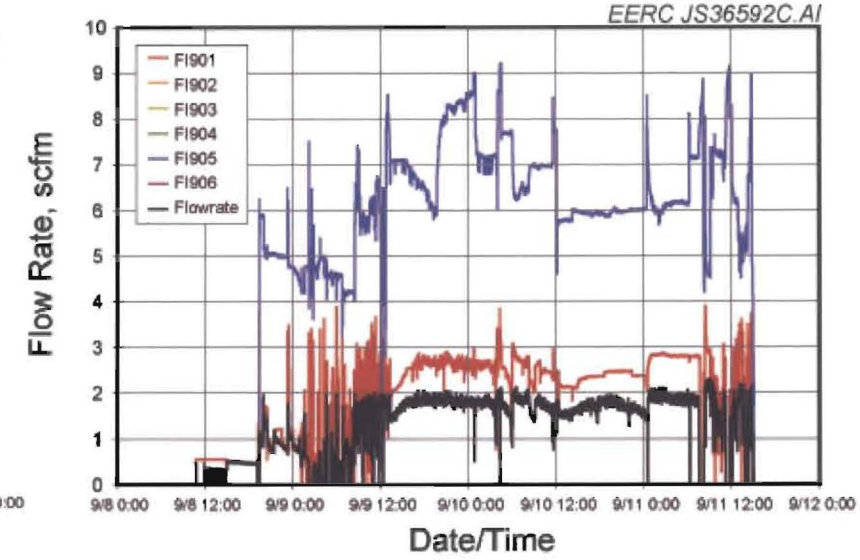

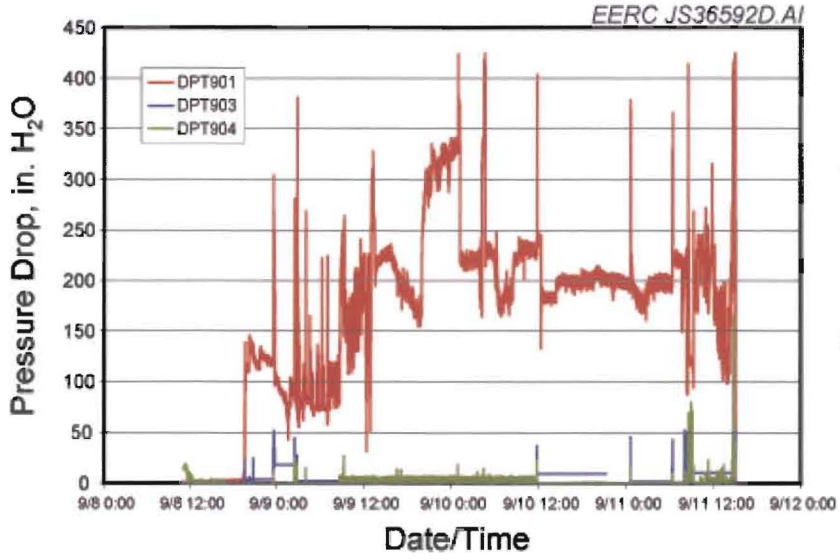
EERC JS36592D.AI
Pressure Drop, in. H_2O
DPT901
DPT903
DPT904
450
400
350
300
250
200
150
100
50
0
9/8 0:00
9/8 12:00
9/9 0:00
9/9 12:00
9/10 0:00
9/10 12:00
9/11 0:00
9/11 12:00
9/12 0:00
Date/Time

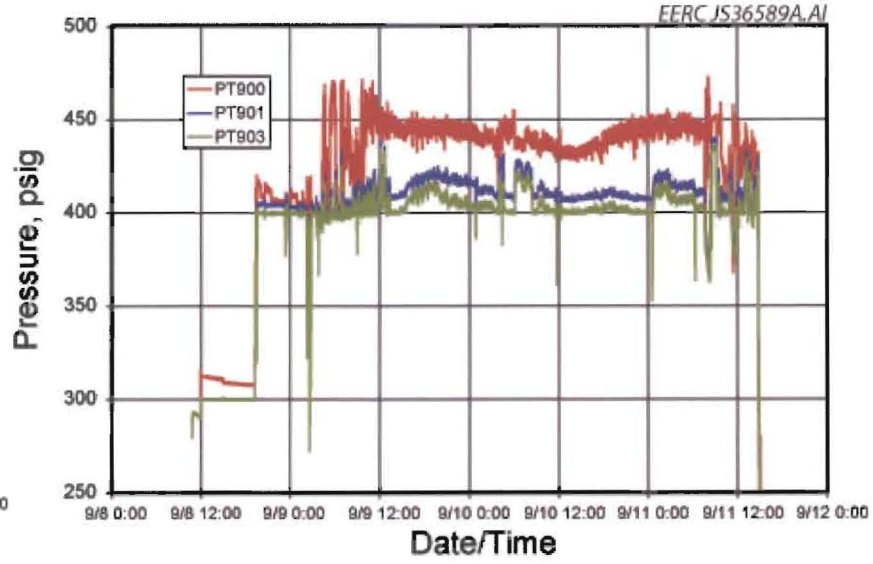
EERC JS36589A.AI
Pressure, psig
PT900
PT901
PT903
500
450
400
350
300
250
9/8 0:00
9/8 12:00
9/9 0:00
9/9 12:00
9/10 0:00
9/10 12:00
9/11 0:00
9/11 12:00
9/12 0:00
Date/Time

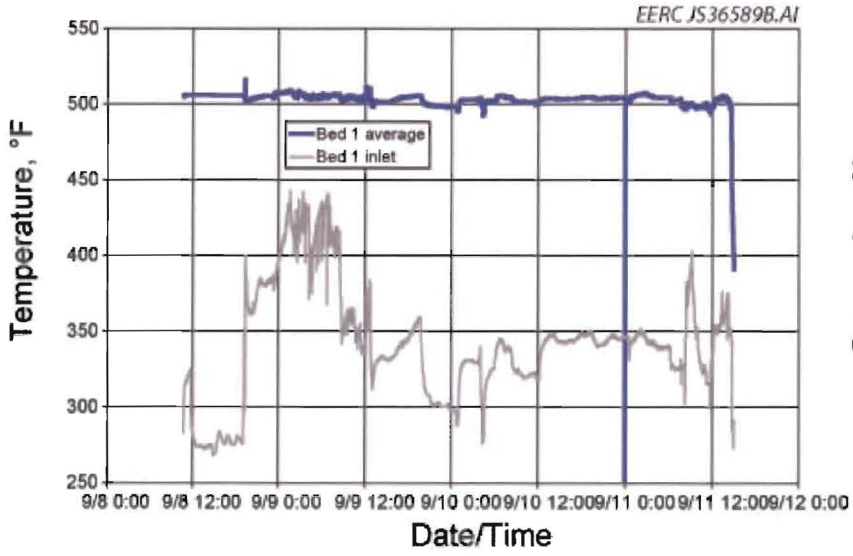
EERC JS36589B.AI
Temperature, °F
Bed 1 average
Bed 1 inlet
550
500
450
400
350
300
250
9/8 0:00
9/8 12:00
9/9 0:00
9/9 12:00
9/10 0:00
9/10 12:00
9/11 0:00
9/11 12:00
9/12 0:00
Date/Time

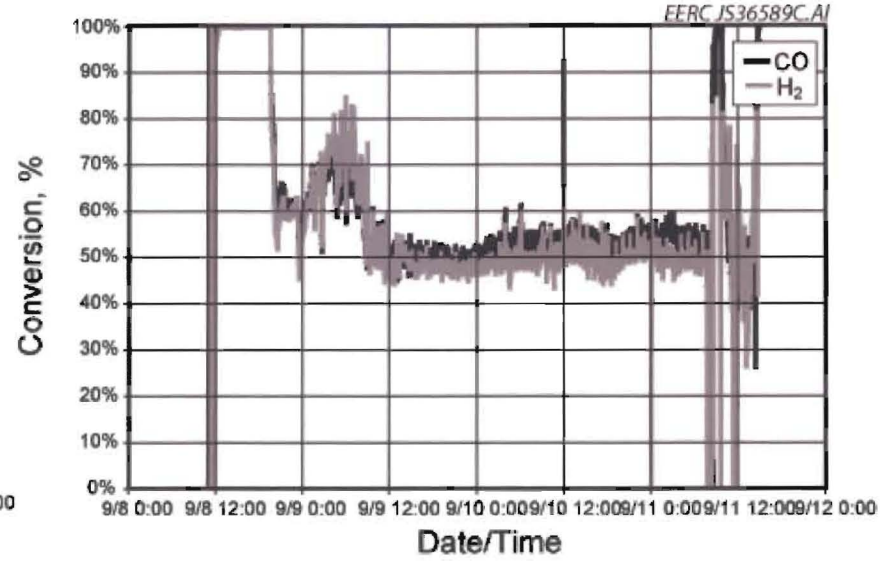
EERC JS36589C.AI
Conversion, %
CO
H_2
100%
90%
80%
70%
60%
50%
40%
30%
20%
10%
0%
9/8 0:00
9/8 12:00
9/9 0:00
9/9 12:00
9/10 0:00
9/10 12:00
9/11 0:00
9/11 12:00
9/12 0:00
Date/Time

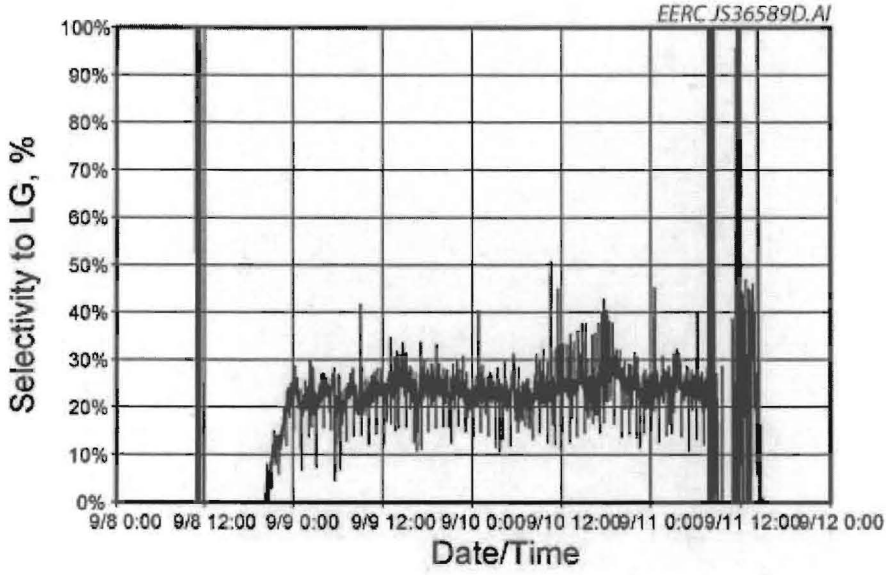
EERC JS36589D.AI
Selectivity to LG, %
100%
90%
80%
70%
60%
50%
40%
30%
20%
10%
0%
9/8 0:00
9/8 12:00
9/9 0:00
9/9 12:00
9/10 0:00
9/10 12:00
9/11 0:00
9/11 12:00
9/12 0:00
Date/Time

FBG004

Gasifier Trends

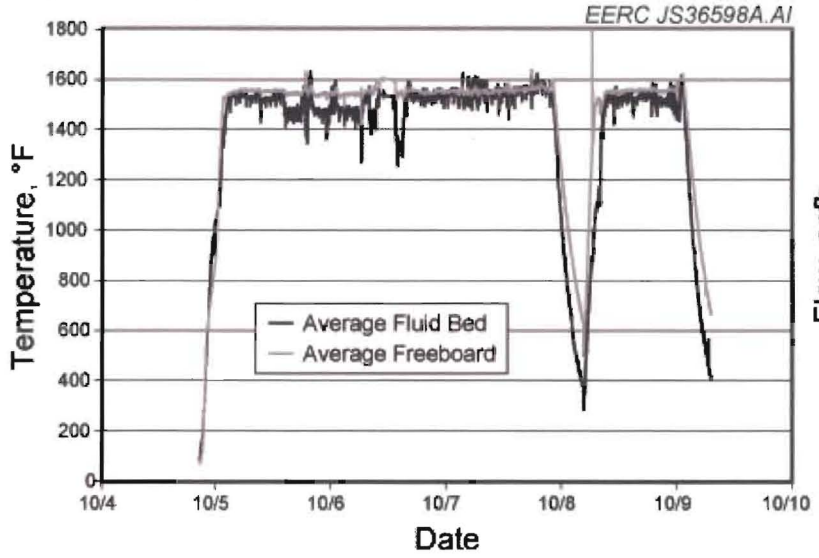

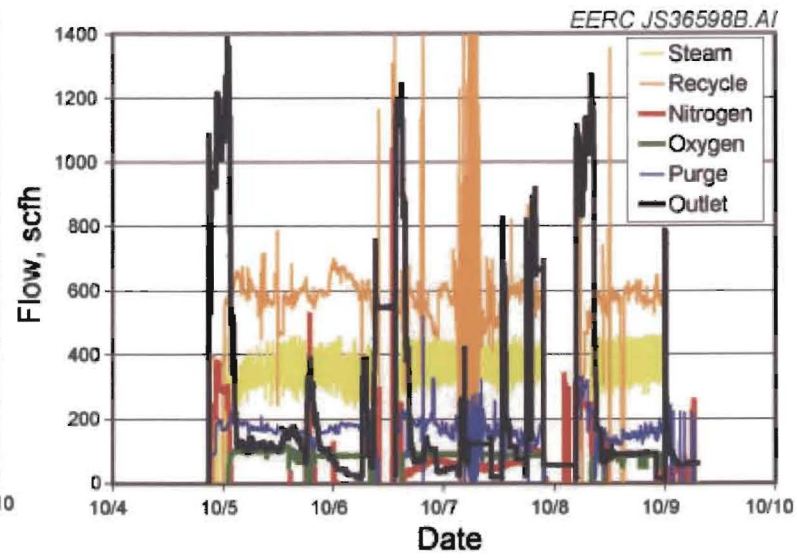

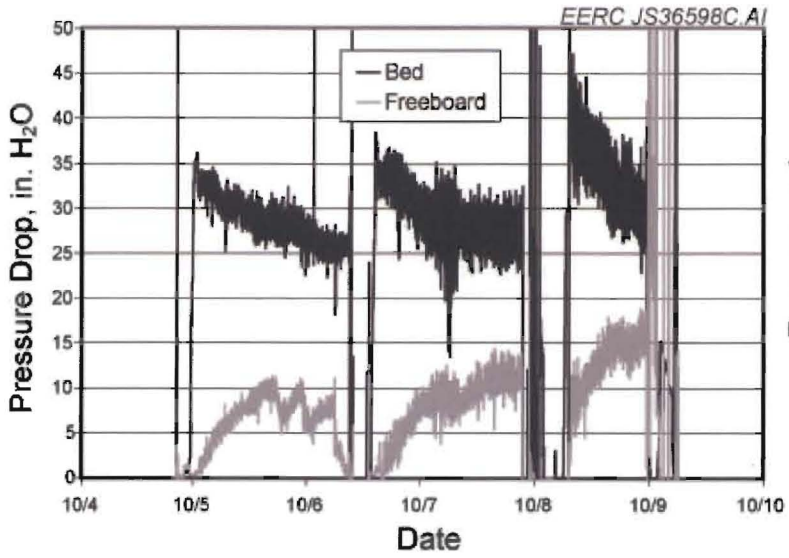

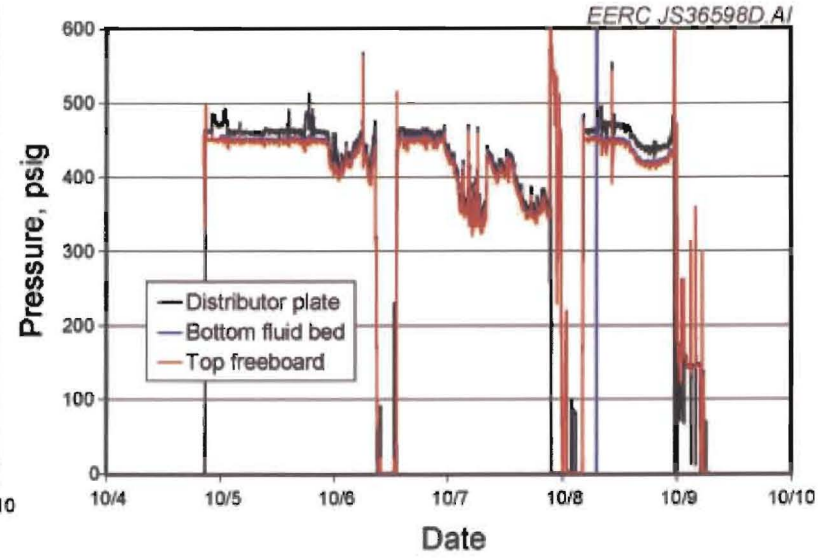

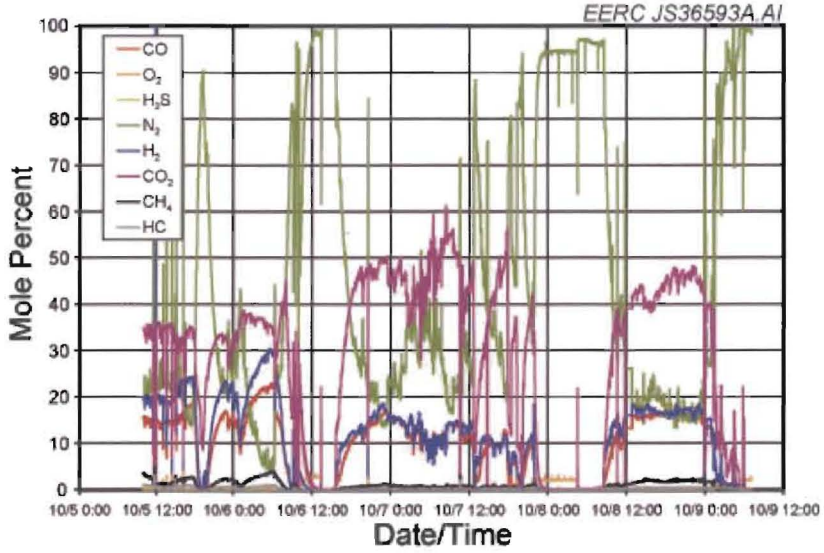

FT Reactor Trends

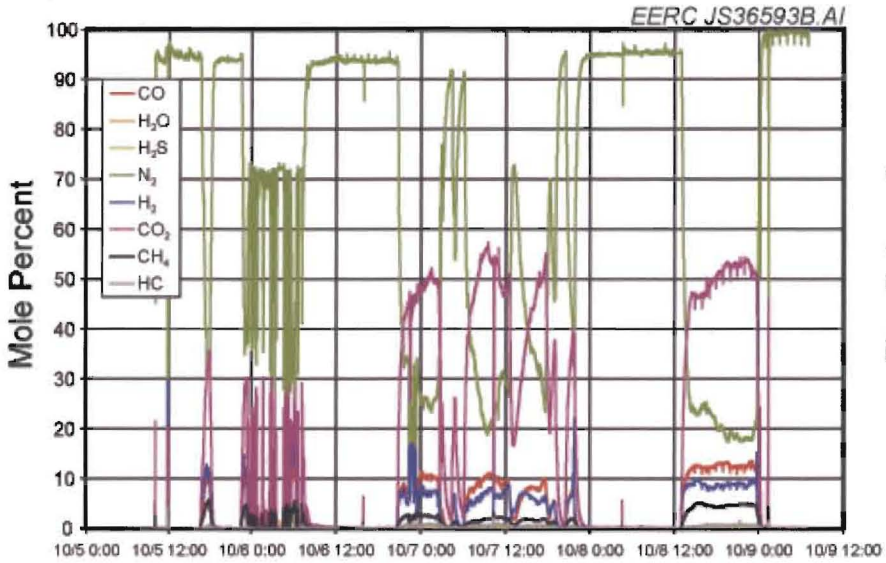

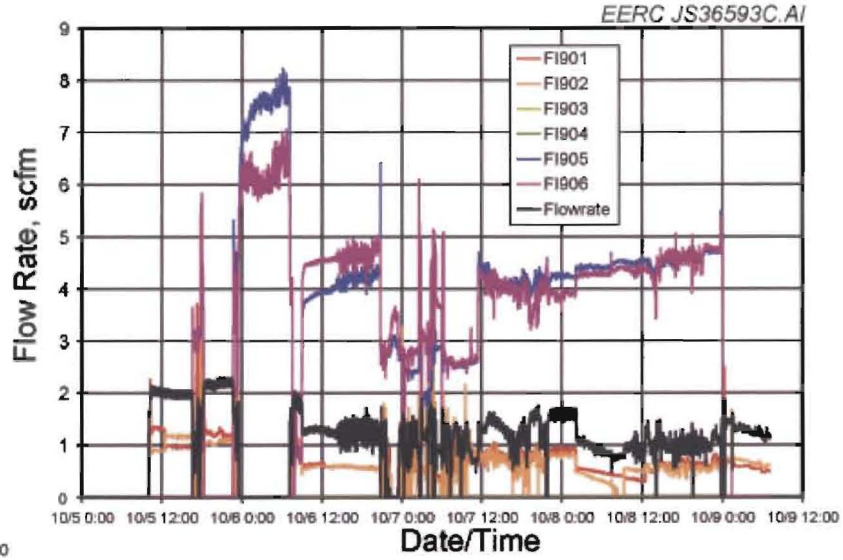

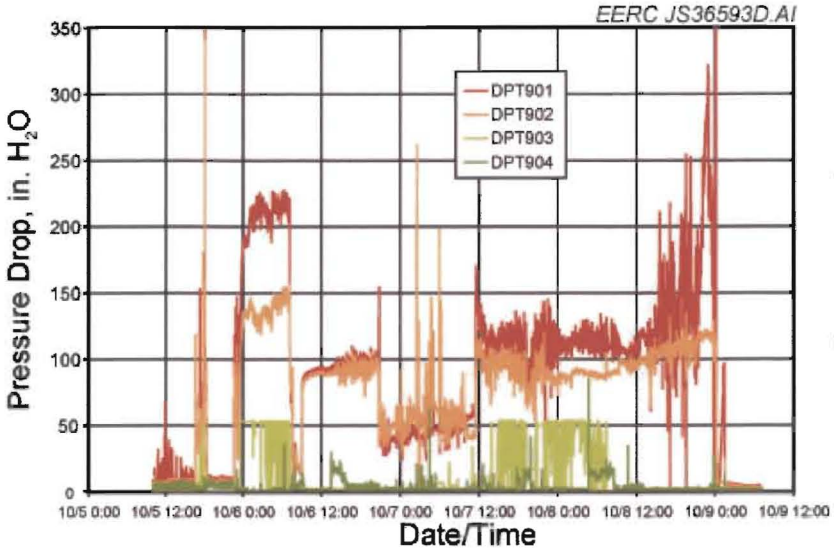
EERC JS36593D.AI
Pressure Drop, in. H_2O
DPT901
DPT902
DPT903
DPT904
350
300
250
200
150
100
50
0
10/5 0:00 10/5 12:00 10/6 0:00 10/6 12:00 10/7 0:00 10/7 12:00 10/8 0:00 10/8 12:00 10/9 0:00 10/9 12:00
Date/Time

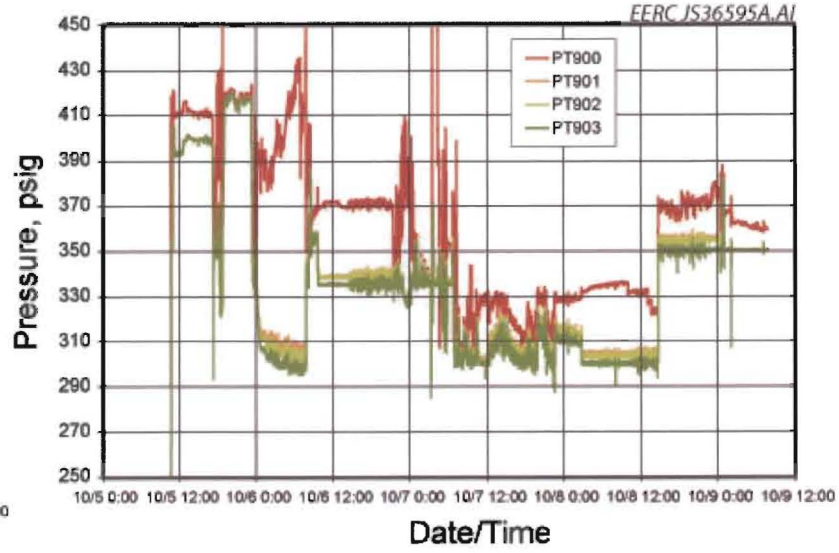
EERC JS36595A.AI
Pressure, psig
PT900
PT901
PT902
PT903
450
430
410
390
370
350
330
310
290
270
250
10/5 0:00 10/5 12:00 10/6 0:00 10/6 12:00 10/7 0:00 10/7 12:00 10/8 0:00 10/8 12:00 10/9 0:00 10/9 12:00
Date/Time

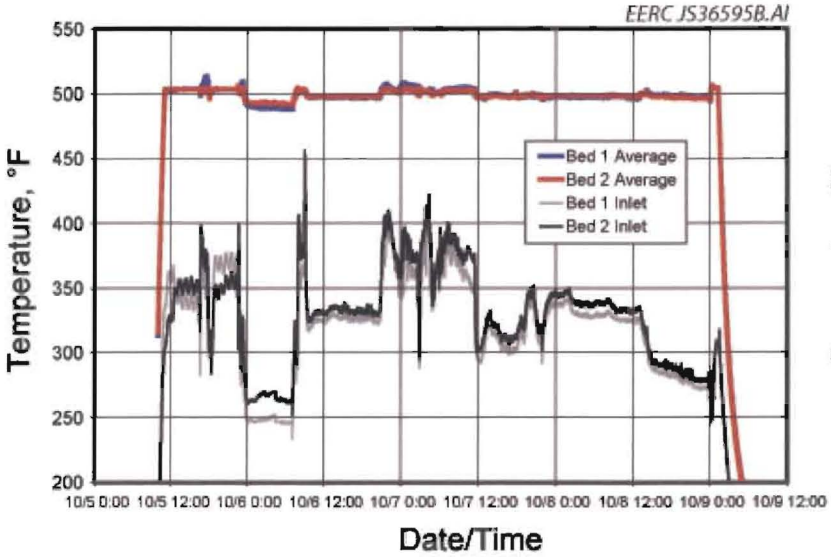
EERC JS36595B.AI
Temperature, °F
Bed 1 Average
Bed 2 Average
Bed 1 Inlet
Bed 2 Inlet
550
500
450
400
350
300
250
200
10/5 0:00 10/5 12:00 10/6 0:00 10/6 12:00 10/7 0:00 10/7 12:00 10/8 0:00 10/8 12:00 10/9 0:00 10/9 12:00
Date/Time

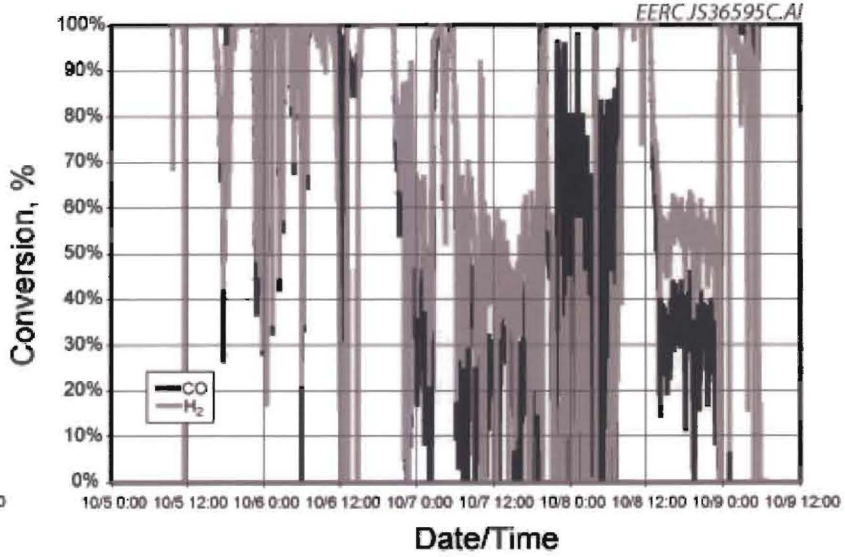
EERC JS36595C.AI
Conversion, %
CO
H_2
100%
90%
80%
70%
60%
50%
40%
30%
20%
10%
0%
10/5 0:00 10/5 12:00 10/6 0:00 10/6 12:00 10/7 0:00 10/7 12:00 10/8 0:00 10/8 12:00 10/9 0:00 10/9 12:00
Date/Time

EERC/S36595D.AI
Selectivity to LG, %
100%
90%
80%
70%
60%
50%
40%
30%
20%
10%
0%
10/5 0:00
10/5 12:00
10/6 0:00
10/6 12:00
10/7 0:00
10/7 12:00
10/8 0:00
10/8 12:00
10/9 0:00
10/9 12:00
Date/Time

FBG005
Gasifier Trends

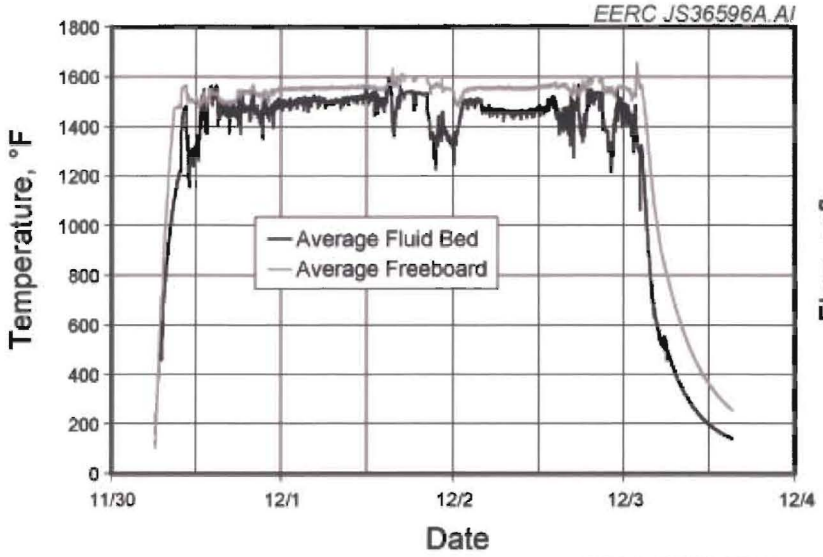

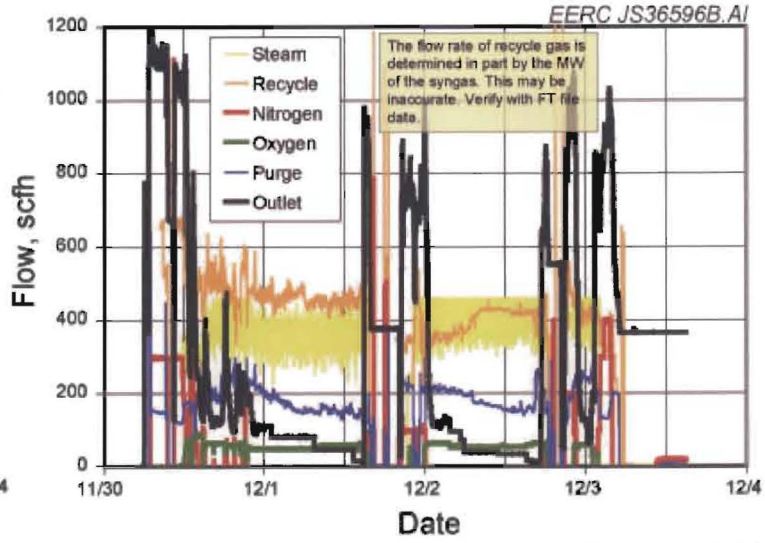

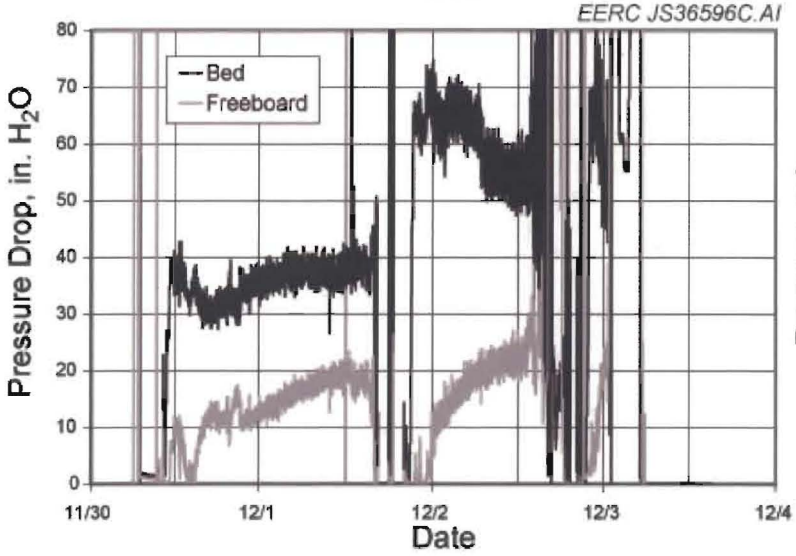

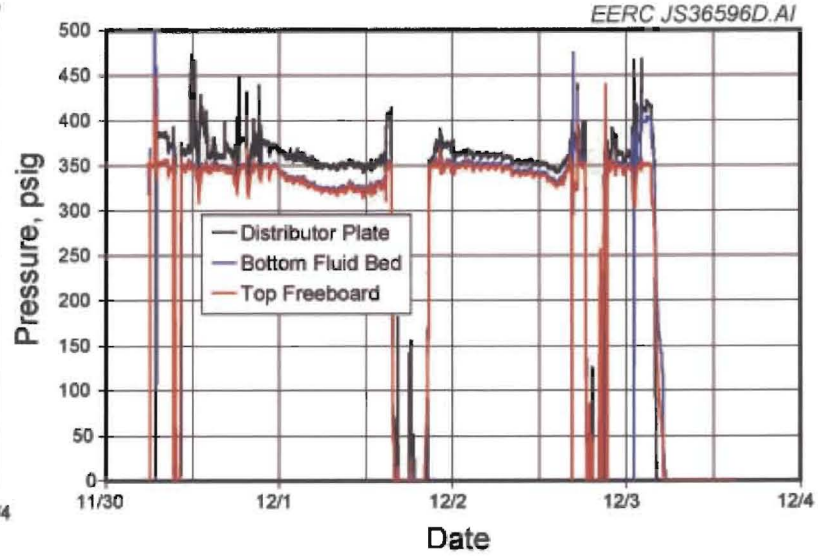

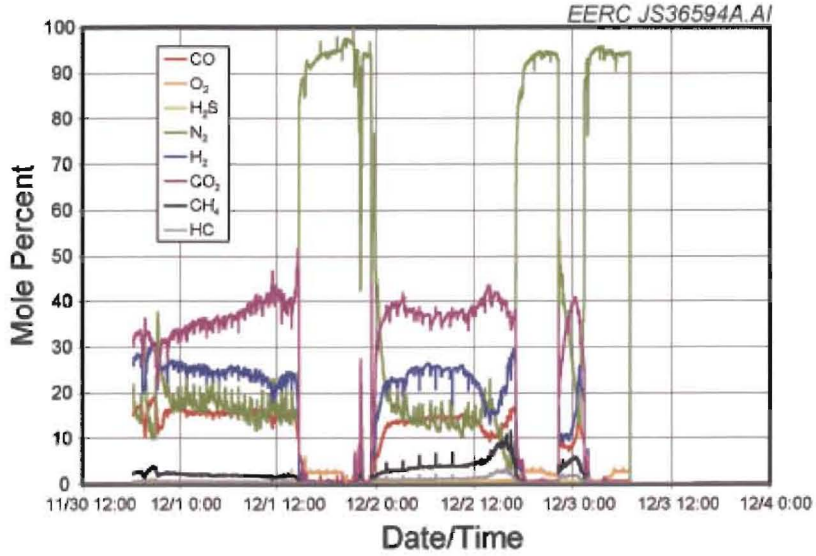

FT Reactor Trends

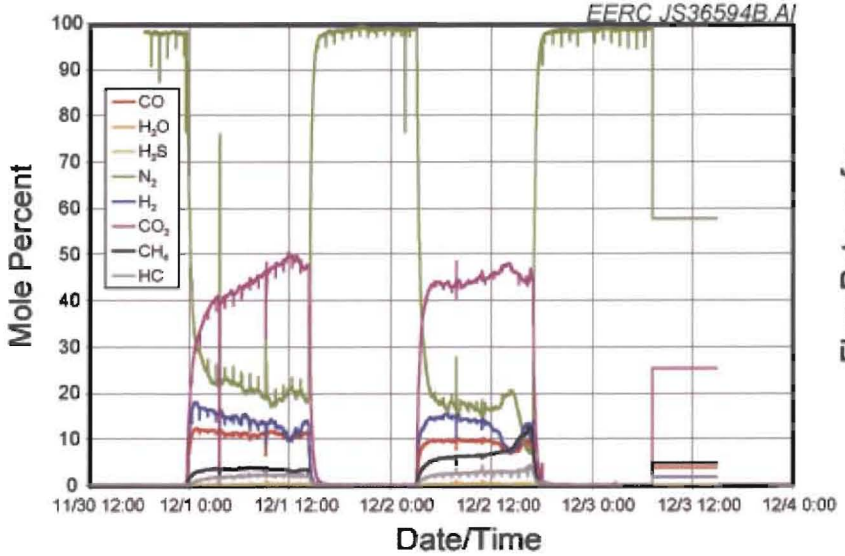

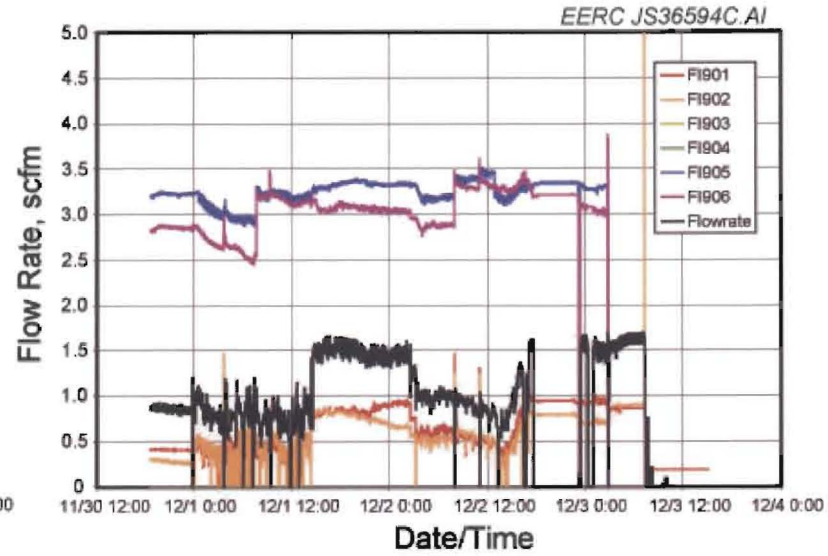

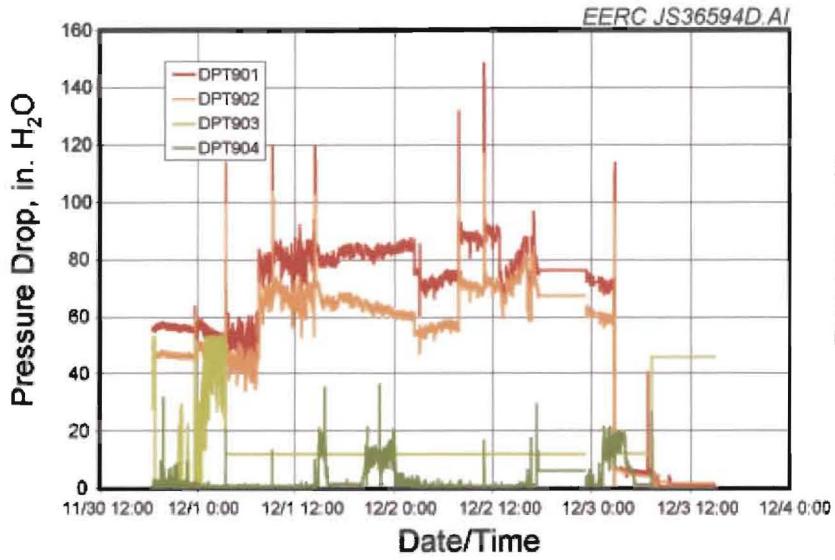
EERC JS36594D.AI
Pressure Drop, in. H_2O
DPT901
DPT902
DPT903
DPT904
160
140
120
100
80
60
40
20
0
11/30 12:00
12/1 0:00
12/1 12:00
12/2 0:00
12/2 12:00
12/3 0:00
12/3 12:00
12/4 0:00
Date/Time

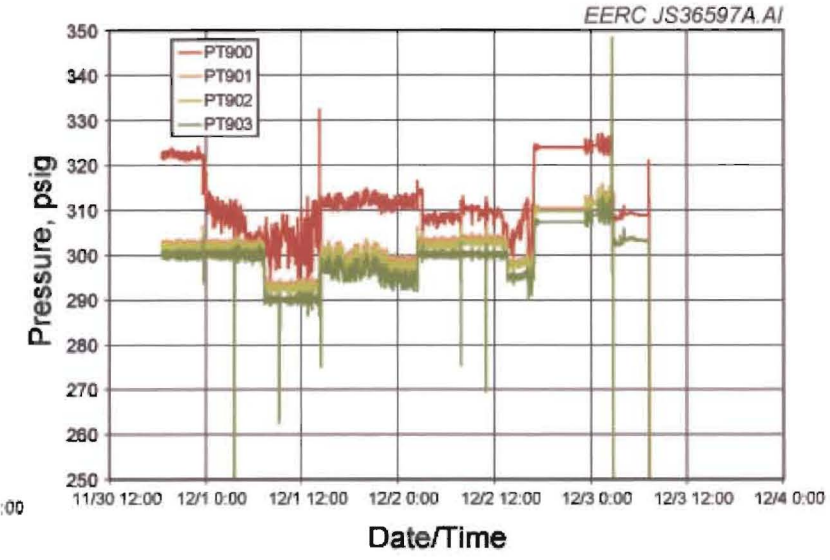
EERC JS36597A.AI
Pressure, psig
PT900
PT901
PT902
PT903
350
340
330
320
310
300
290
280
270
260
250
11/30 12:00
12/1 0:00
12/1 12:00
12/2 0:00
12/2 12:00
12/3 0:00
12/3 12:00
12/4 0:00
Date/Time

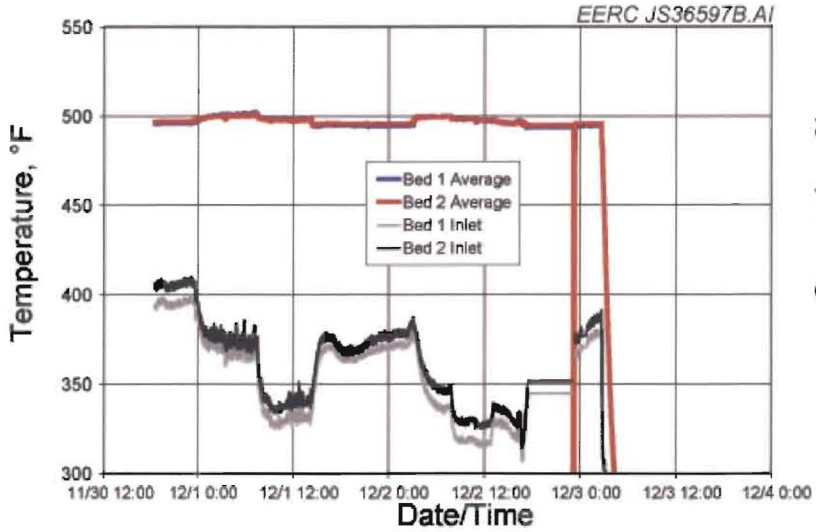
EERC JS36597B.AI
Temperature, °F
Bed 1 Average
Bed 2 Average
Bed 1 Inlet
Bed 2 Inlet
550
500
450
400
350
300
11/30 12:00
12/1 0:00
12/1 12:00
12/2 0:00
12/2 12:00
12/3 0:00
12/3 12:00
12/4 0:00
Date/Time

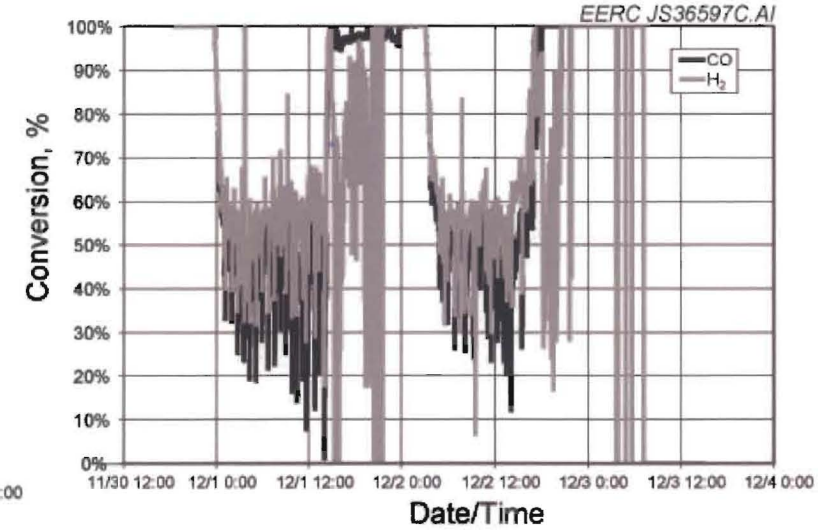
EERC JS36597C.AI
Conversion, %
CO
H_2
100%
90%
80%
70%
60%
50%
40%
30%
20%
10%
0%
11/30 12:00
12/1 0:00
12/1 12:00
12/2 0:00
12/2 12:00
12/3 0:00
12/3 12:00
12/4 0:00
Date/Time

EERC
Energy & Environmental Research Center

APPENDIX B

DESCRIPTION OF EQUIPMENT

Printed on Recycled Paper

DESCRIPTION OF EQUIPMENT

FLUID-BED GASIFIER

The Energy & Environmental Research Center's (EERC's) high-pressure fluid-bed gasifier (FBG) is capable of feeding up to 9.0 kg/hr (20 lb/hr) of pulverized coal or biomass at pressures up to 70 bar absolute (1000 psig). The externally heated bed is initially charged from an independent hopper with silica sand or, in the case of high-alkali fuels, an appropriate fluidization media. Independent mass flow controllers meter the flow of nitrogen, oxygen, steam, and recycled syngas into the bottom of the fluid bed. Various safety interlocks prevent the inadvertent flow of pure oxygen into the bed or reverse flow into the coal feeder.

After a review of available alloys, Haynes 556® was selected as the material most suitable for fabrication of the high-temperature, high-pressure system as well as for all of the reactor nozzles and the cyclone. The reactor was designed with the capability to operate at a maximum operating pressure (MOP) of 1000 psig at an operational temperature of 1550°F, 650 psig at an operational temperature of 1650°F, and 300 psig at an operational temperature of 1800°F. The 2500-pound 316H stainless steel flanged connections at the top and bottom of the reactor are limited to somewhat lower maximum operating temperatures but do not greatly impact the operation of the gasifier, as they are generally cooler than the reactor bed itself. A design drawing of the reactor is shown in Figure B-1, and a photograph of the gasifier is shown in Figure B-2. Although omitted from the drawing for clarity, 16 thermocouple ports are spaced every 4–5 inches up the bed to monitor for loss of fluidization, solids agglomeration, and localized combustion zones, and the feed line extends up two stories to the coal hopper.

Coal is fed from a pressurized K-tron® loss-in-weight feeder that provides online measurement of coal feed rate at pressures up to 1000 psig. This system (shown schematically in Figure B-3) allows instantaneous measurement of the fuel feed rate to the gasification system. The feed system electronic controls are interfaced to a data acquisition system that allows for local or remote computer control of the fuel feed rate. Above the main feed hopper is the fuel charge hopper. The fuel charge hopper is manually charged with fuel through the top valve while at atmospheric pressure. It is then sealed and pressurized. Finally, the fuel feed material is transferred by gravity feed to the weigh hopper inside through the lower dual-valve system. The entire feed system pressure vessel is on a movable platform to allow easy transition from the FBG to the EERC's entrained-flow gasifier (not used in this testing but located adjacent to the FBG).

Coal feed from the K-tron system drops through a long section of vertical tubing and is then pushed quickly into the fluid bed through a downward-angled feed auger, as seen in Figures B-1 and B-2. Syngas exiting the fluid bed passes through a cyclone before flowing into a transport reactor that uses regenerable sorbent to remove sulfur from the syngas stream. The syngas then passes through a hot candle filter to remove fine particulate before entering a series of fixed beds. One bed is a polishing bed of ZnO that removes all remaining traces of sulfur from the syngas. Other beds can be loaded with water–gas shift catalyst, heavy metal sorbent, a chlorine guard, or other sorbents and catalysts. The clean, shifted syngas, still hot and

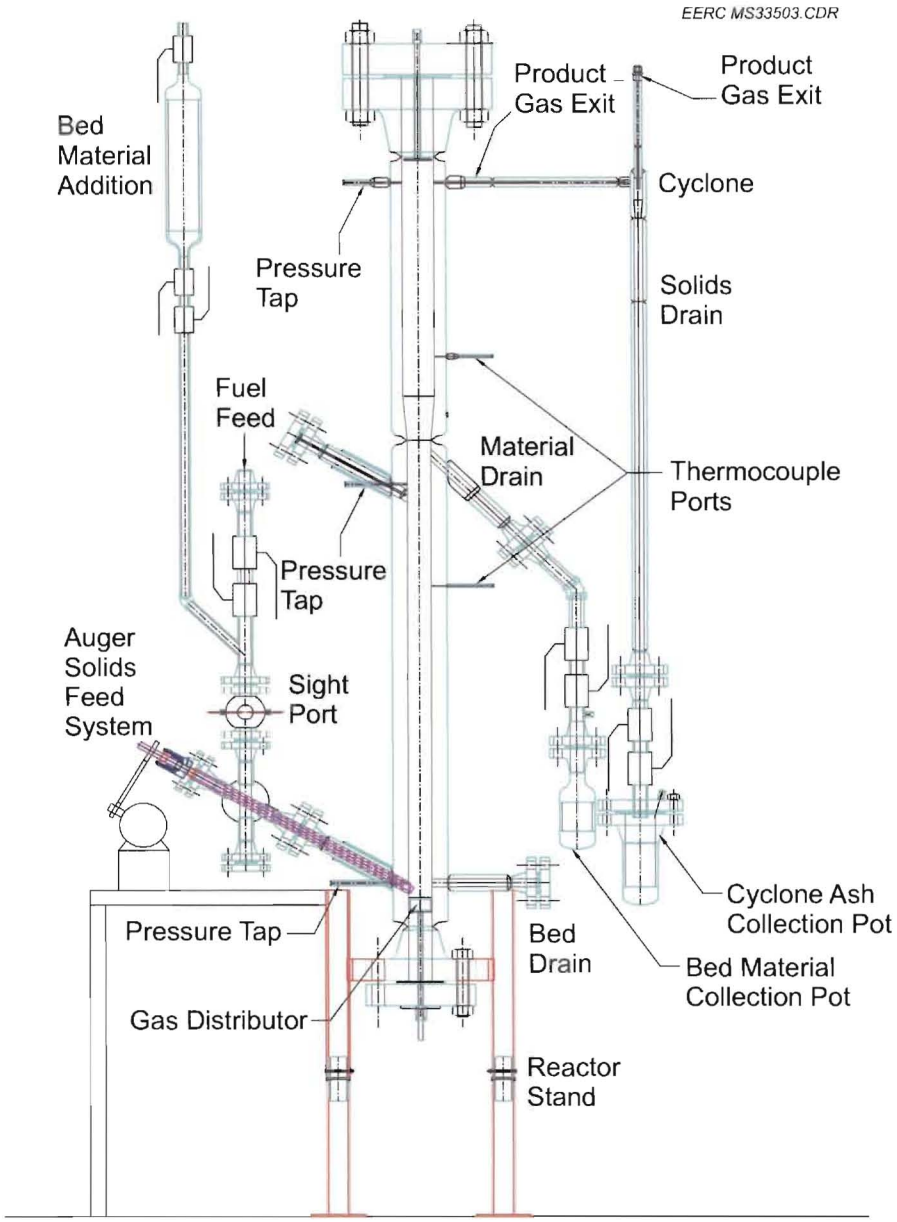

Figure B-1. Design drawing of the pressurized, fluidized-gasification reactor.

pressurized, is then routed through a series of water-cooled condensers to remove volatile organics and moisture. Syngas can be sampled upstream of the condensers for hot tests. The clean, dry syngas exiting the condensers is then recycled through a compressor to the bottom of the FBG, and a portion is vented through a control valve to maintain system pressure. The syngas exiting the system passes through a dry gas meter for mass balance. A slipstream of this depressurized, dry gas is also fed to a laser gas analyzer and a gas chromatograph for online analysis of major gas components and for low-level (ppb) analysis of sulfur species. In addition, operators periodically sample syngas from various points throughout the system using Dräger tubes for H_2S and other trace gases to verify low-level chromatograph data.

Figure B-2. Photograph of the lower section of high-pressure FBG. Visible at left is the feed auger angled downward into the bed.

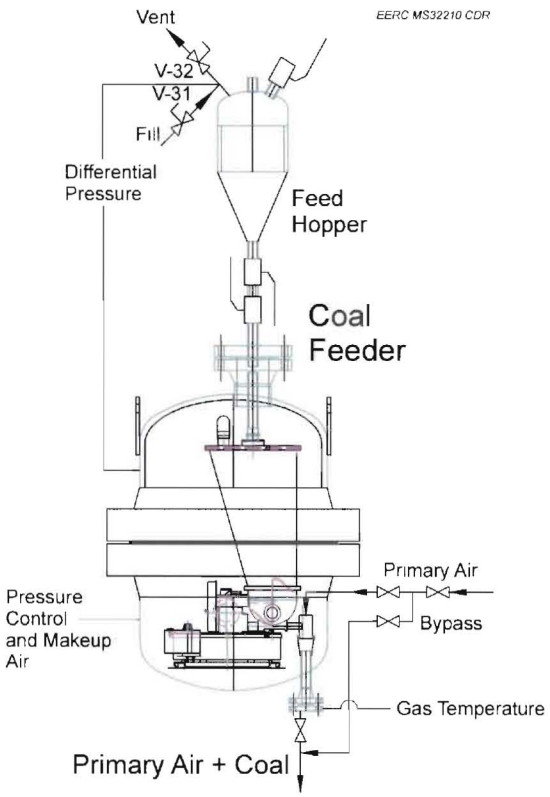

Figure B-3. Cross-sectional view of the fuel feed system.

Figure B-4 depicts a piping and instrumentation diagram (P&ID) of the back-end gas cleanup system, including the transport sulfur reactor, filter vessel, fixed sorbent/catalyst beds, and quench system.

FISCHER–TROPSCH (FT) REACTOR

Pressurized syngas exiting the fluid-bed system can be routed to several back-end systems, one of which is a FT reactor with an estimated liquid production rate of 4 L (1 gal) per day per reactor bed. The FT reactor system meters up to 3.5 scfm per bed of clean, pressure-regulated syngas from the FBG through a preheater and then into a set of down-flow, parallel, packed shell-and-tube reactor beds. Two reactor beds are currently installed on the system, with room for expansion to four. The reactor beds can operate at up to 1000 psig and 570°F, allowing the possibility of methanol or mixed alcohol synthesis in future tests.

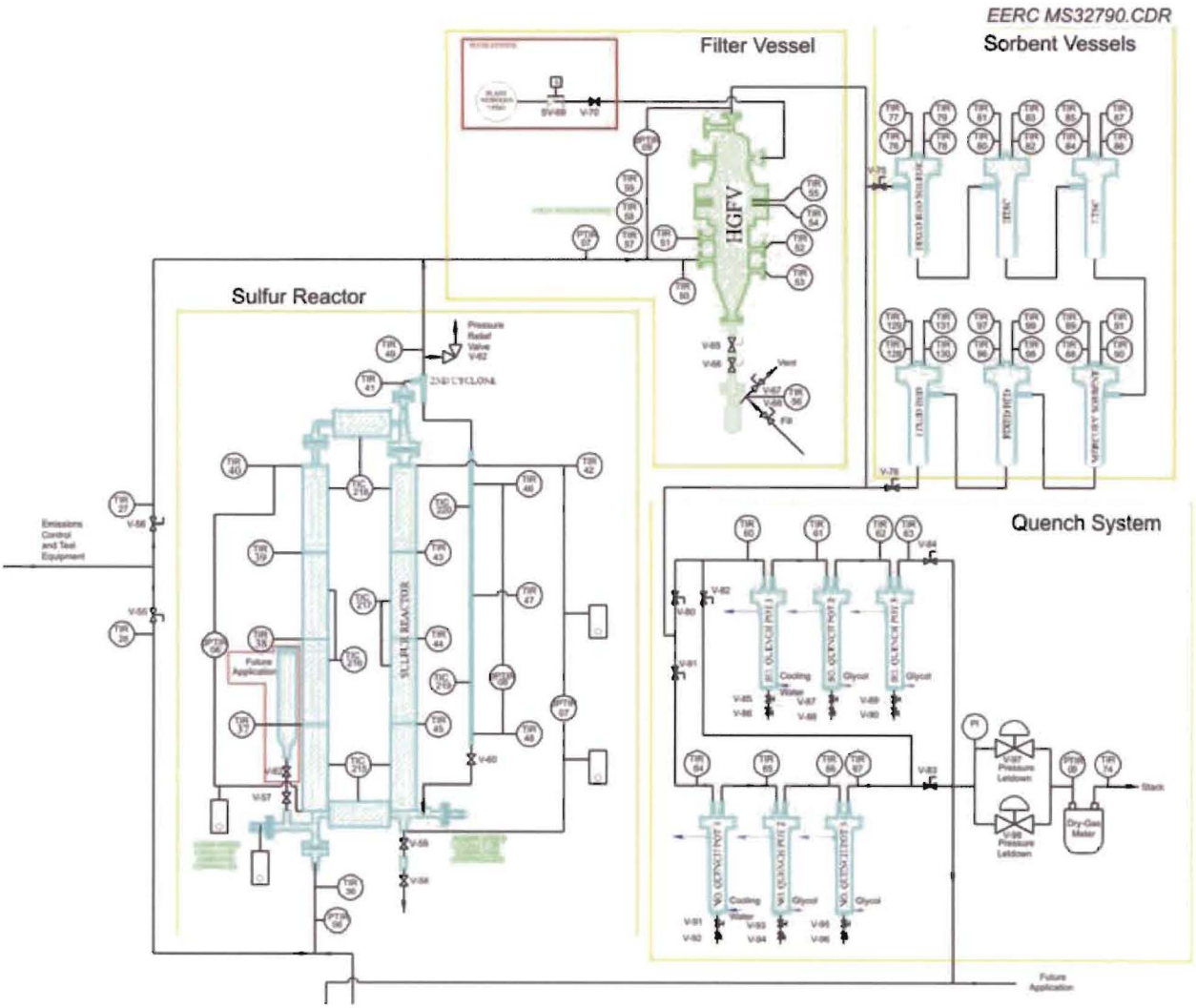

Figure B-4. P&ID for the gas cleanup system.

The shell-and-tube reactor beds are initially heated to temperature using a countercurrent flow of Dowtherm through the external (shell-side) tube. Syngas passing through the beds is then slowly brought to operating pressure, which begins the exothermic FT reaction. As pressure builds and the beds begin to heat under exothermic reaction, the Dowtherm heater is turned down and the Dowtherm begins to function as a coolant. Because the packed-bed design lends itself to runaway exotherms, single-pass conversion is kept low, and product gas exiting the beds is recycled through preheater coils to the bed inlets. This dilutes incoming syngas and achieves higher overall conversion efficiencies. Liquid exiting the bottom of the packed beds is collected in a heated wax trap before passing through a set of water-cooled condensers to remove lighter organic material and water. Hot liquid in the wax trap can be recycled to the top of the reactor to provide further syngas dilution and catalyst cooling, thus bringing the inlet to the packed beds closer to outlet conditions. This design allows the packed beds to function similarly to slurry bed designs more commonly used in large-scale FT synthesis. Unrecycled product gas is depressurized and measured through a dry gas meter, and a slipstream is passed to a laser gas analyzer to provide online comparison of inlet syngas and outlet product gas composition.

Figure B-5 is a photograph of the FT reactor system. Because the entire unit is compact and skid-mounted, it can be readily moved to any of the different gasification systems located at the EERC or can be loaded into a truck and coupled to an off-site gasifier. This design flexibility in terms of recycle ratio, operating conditions, heat load or heat removal, and placement makes the FT reactor system a valuable tool for testing catalysts under a wide variety of scenarios.

Figure B-5. Photograph of EERC FT reactor.